Selective transport of neurotransmitters and modulators by distinct volume-regulated LRRC8 anion channels

Lutter, D., Ullrich, F., Lueck, J.C., Kempa, S., Jentsch, T.J.

Journal of Cell Science
2017 MAR 15 ; 130(6): 1122-1133
2017 FEB 12 (First published online: final version)
doi: 10.1242/jcs.196253

Publisher: The Company of Biologists Ltd.

© 2017. Published by The Company of Biologists Ltd | Journal of Cell Science (2017) 130, 1122-1133 doi:10.1242/jcs.196253

RESEARCH ARTICLE

Selective transport of neurotransmitters and modulators by distinct volume-regulated LRRC8 anion channels

Darius Lutter[1,2,3], Florian Ullrich[1,2], Jennifer C. Lueck[1,2,3], Stefan Kempa[2] and Thomas J. Jentsch[1,2,4,*]

ABSTRACT

In response to swelling, mammalian cells release chloride and organic osmolytes through volume-regulated anion channels (VRACs). VRACs are heteromers of LRRC8A and other LRRC8 isoforms (LRRC8B to LRRC8E), which are co-expressed in HEK293 and most other cells. The spectrum of VRAC substrates and its dependence on particular LRRC8 isoforms remains largely unknown. We show that, besides the osmolytes taurine and *myo*-inositol, LRRC8 channels transport the neurotransmitters glutamate, aspartate and γ-aminobutyric acid (GABA) and the co-activator D-serine. HEK293 cells engineered to express defined subsets of LRRC8 isoforms were used to elucidate the subunit-dependence of transport. Whereas LRRC8D was crucial for the translocation of overall neutral compounds like *myo*-inositol, taurine and GABA, and sustained the transport of positively charged lysine, flux of negatively charged aspartate was equally well supported by LRRC8E. Disruption of LRRC8B or LRRC8C failed to decrease the transport rates of all investigated substrates, but their inclusion into LRRC8 heteromers influenced the substrate preference of VRAC. This suggested that individual VRACs can contain three or more different LRRC8 subunits, a conclusion confirmed by sequential co-immunoprecipitations. Our work suggests a composition-dependent role of VRACs in extracellular signal transduction.

KEY WORDS: VSOAC, VSOR, Swelling-activated chloride channel, $I_{Cl,vol}$, $I_{Cl,swell}$, Gliotransmission

INTRODUCTION

Neurons and astrocytes can release neurotransmitters and other signaling molecules not only by vesicular exocytosis, but also through channel-like mechanisms (Hamilton and Attwell, 2010; Harada et al., 2015; Kimelberg et al., 1990; Pasantes-Morales et al., 1994; Verkhratsky et al., 2016, 2012). Several channels have been implicated in channel-like neurotransmitter release, including connexin hemichannels and pannexins (Montero and Orellana, 2015; Orellana and Stehberg, 2014), P2X7 receptors (Duan et al., 2003), bestrophins (Lee et al., 2010), and the volume-regulated anion channel (VRAC) (Kimelberg et al., 1990; Pasantes-Morales et al., 1994).

VRAC [also known as VSOR, volume-stimulated outward rectifier (Okada, 1997)] is a major player in mammalian cell volume regulation (Jentsch, 2016; Nilius et al., 1997; Pedersen et al., 2016). This plasma membrane channel, which appears to be expressed in all cells, is normally closed but can be activated by cell swelling or other cellular signaling cascades. In most cells, VRAC opening leads to an efflux of Cl^-, which, together with an efflux of K^+ through independent K^+ channels, lowers the intracellular osmolarity and, by secondarily driving water efflux, results in regulatory volume decrease. Cell swelling also stimulates an efflux of organic 'osmolytes' such as *myo*-inositol, taurine and glutamate. It was controversial whether this release occurs through VRAC or through a distinct channel named VSOAC (for volume-sensitive organic osmolyte/anion channel) (Jackson and Strange, 1993; Shennan, 2008), but this issue has been resolved recently when LRRC8 proteins were finally identified as constituents of VRAC channels (Qiu et al., 2014; Voss et al., 2014).

VRACs are composed of LRRC8 heteromers of the obligatory subunit LRRC8A (Qiu et al., 2014; Voss et al., 2014) and at least one other LRRC8 isoform (LRRC8B, LRRC8C, LRRC8D or LRRC8E) (Voss et al., 2014). Genomic disruption (Voss et al., 2014) or siRNA-mediated knockdown (Qiu et al., 2014) of LRRC8A not only abolishes the swelling-activated Cl^- current, $I_{Cl,vol}$, but also the efflux of taurine. Cellular taurine release is also abolished in cells lacking all LRRC8 subunits except LRRC8A [denoted *LRRC8(B,C,D,E)*$^{-/-}$] (Voss et al., 2014). Hence, both VRAC and the taurine-conducting 'VSOAC' are composed of LRRC8 heteromers. Furthermore, hypotonicity-induced aspartate efflux (thought to reflect glutamate efflux) is diminished when *LRRC8A* expression is reduced by siRNA transfection (Hyzinski-García et al., 2014).

In addition to being an important osmolyte, the sulfo-amino acid taurine activates inhibitory glycine and, possibly, γ-aminobutyric acid (GABA) receptors (Le-Corronc et al., 2011; Schmieden et al., 1989). It might also serve as a gliotransmitter in central osmoregulation (Choe et al., 2012; Hussy et al., 2000, 1997; Le-Corronc et al., 2011). Glutamate [and to a lesser degree aspartate (Chen et al., 2005; Patneau and Mayer, 1990)] activates excitatory glutamate receptors, with swelling-induced release of glutamate thought to play a role in pathological conditions such as stroke and spreading depression (Akita and Okada, 2014). D-serine, a co-activator of ionotropic glutamate receptors (Mothet et al., 2000), has also been suggested as potential VRAC substrate (Martineau et al., 2014; Rosenberg et al., 2010), whereas there is no clear evidence for VRAC-dependent transport of the inhibitory neurotransmitter GABA (Franco et al., 2001). Disruption of *LRRC8* genes can now be used to stringently assess whether these compounds are transported by VRACs.

The homology of LRRC8 proteins to pannexins and the size of purified heteromers on native gels suggest that VRACs may be hexameric complexes of LRRC8 proteins (Abascal and Zardoya, 2012; Syeda et al., 2016; Voss et al., 2014). Together with the presence of five different *LRRC8* genes, which are often co-expressed in the same cell, a hexameric assembly suggests that there

[1]Leibniz-Institut für Molekulare Pharmakologie (FMP), D-13125 Berlin, Germany. [2]Max-Delbrück-Centrum für Molekulare Medizin (MDC), D-13125 Berlin, Germany. [3]Graduate Program of the Freie Universität Berlin, D-14195 Berlin, Germany. [4]Neurocure, Charité Universitätsmedizin, D-10117 Berlin, Germany.

*Author for correspondence (Jentsch@fmp-berlin.de)

T.J.J., 0000-0002-3509-2553

Received 1 August 2016; Accepted 31 January 2017

Journal of Cell Science (2017) 130, 1122-1133 doi:10.1242/jcs.196253

could be a large number of differently composed VRAC channels that may have different properties. Indeed, the LRRC8 subunit composition determines the voltage-dependent inactivation of VRAC currents at non-physiological, inside-positive potentials (Ullrich et al., 2016; Voss et al., 2014), and their single-channel amplitudes (Syeda et al., 2016). Furthermore, the LRRC8D subunit is crucial for the VRAC-mediated cellular uptake of blasticidin S (Lee et al., 2014) and of the anti-cancer drugs cisplatin and carboplatin (Planells-Cases et al., 2015). It is also crucial for the swelling-induced efflux of taurine (Planells-Cases et al., 2015). However, the subunit-dependence of other organic VRAC substrates remains unclear despite their potential importance in extracellular signaling.

We now use HEK293 cell lines carrying genomic disruptions of individual *LRRC8* genes to rigorously test whether previously postulated VRAC/VSOAC substrates are indeed transported by LRRC8 heteromers and whether their transport depends on specific LRRC8 subunits. While also studying the uncharged osmolyte *myo*-inositol and positively charged lysine, we mainly focus on neurotransmitters and modulators that were previously discussed as VRAC substrates. Moreover, we show that GABA, the main inhibitory neurotransmitter in the mammalian brain, permeates through VRACs. The LRRC8 subunit-dependence of organic substance transport suggests that disruption of specific LRRC8 isoforms may be useful to elucidate the importance of VRAC-dependent neurotransmitter transport in health and disease.

RESULTS

VRACs transport several neurotransmitters and neuromodulators

Wild-type (WT) and *LRRC8A*$^{-/-}$ HEK293 cells were loaded with ^{3}[H]D-aspartate, ^{3}[H]D-lysine, ^{3}[H]D-serine, ^{3}[H]GABA, ^{3}[H]taurine and ^{3}[H]*myo*-inositol and subsequently exposed to hypo-osmotic medium to open swelling-activated channels. We determined their efflux by measuring the radioactivity of the supernatant, assuming that these compounds have not been significantly metabolized during the procedure. This assumption is reasonable for the D-amino acids, taurine and *myo*-inositol. For ^{3}[H]GABA efflux experiments we inhibited GABA metabolism with the GABA transaminase inhibitor vigabatrin. Although ^{3}[H]D-aspartate has been widely used as non-metabolizable analog of L-glutamate, we additionally assessed the efflux of endogenous L-glutamate by determining its concentration in the supernatant with an enzymatic assay.

The efflux of all tested substances was strongly increased by hypotonic cell swelling (Fig. 1). The hypotonicity-induced flux component was drastically reduced or abolished in *LRRC8A*$^{-/-}$ cells, demonstrating that this component depends overwhelmingly or exclusively on VRACs. As an exception, there may be a small VRAC-independent component of swelling-induced *myo*-inositol release (Figs 1G and 2). We conclude that besides the glycine-receptor agonist taurine (Planells-Cases et al., 2015; Qiu et al., 2014; Voss et al., 2014), LRRC8 channels can transport several other neuroactive substances, including the major neurotransmitters glutamate and GABA.

LRRC8D and LRRC8E are important for the transport of organic molecules

We next asked which other LRRC8 subunits are required or, together with LRRC8A, sufficient for the transport of these VRAC substrates. The efflux of radiolabeled organic compounds was studied with HEK293 cells lacking single LRRC8 subunits (*LRRC8A*$^{-/-}$, *LRRC8B*$^{-/-}$, …, *LRRC8E*$^{-/-}$ cells) or carrying disruptions in three *LRRC8* genes, resulting in cells expressing LRRC8A together with one other LRRC8 subunit [e.g. *LRRC8(B,C,E)*$^{-/-}$ cells expressing only LRRC8A and LRRC8D]. For each substrate, maximal rates of hypotonicity-induced efflux were normalized to those of WT cells (Fig. 2; a complete timecourse of efflux shown in Fig. S1).

Not only the obligate VRAC subunit LRRC8A, but also LRRC8D played a crucial role in the transport of all tested organic compounds. Swelling-induced taurine efflux was almost absent from *LRRC8D*$^{-/-}$ cells (Planells-Cases et al., 2015) (Fig. 2A). Lack of LRRC8D also almost abolished VRAC-dependent transport of GABA and *myo*-inositol, and markedly reduced the efflux of D-aspartate (Fig. 2A). Conversely, *LRRC8(B,C,E)*$^{-/-}$ cells expressing only LRRC8A and LRRC8D showed substantial transport of all tested compounds, with taurine, GABA and *myo*-inositol efflux reaching or even exceeding WT levels (Fig. 2B).

Disruption of LRRC8E markedly decreased the swelling-induced efflux of D-aspartate, but not of GABA, taurine or *myo*-inositol (Fig. 2A). Conversely, channels containing only LRRC8A and LRRC8E subunits in a heteromeric complex of unknown and possibly variable stoichiometry (denoted LRRC8A/E; hereafter, the forward slash is used to denote the subunits present in the heteromers) enabled a substantial efflux of D-aspartate, but not of the other tested organic compounds (Fig. 2B).

By contrast, neither disruption of *LRRC8B* nor of *LRRC8C* markedly reduced the efflux of any of the tested compounds (Fig. 2A). Moreover, neither LRRC8A/B nor LRRC8A/C heteromers conspicuously supported their transport (with LRRC8A/C heteromers enabling aspartate and taurine transport to a minor degree, Fig. 2B).

Given the important roles of LRRC8D and LRRC8E in the transport of organic compounds, we next studied *LRRC8(B,C)*$^{-/-}$ cells expressing LRRC8A together with both LRRC8D and LRRC8E (Fig. 3A), or *LRRC8(D,E)*$^{-/-}$ cells lacking both LRRC8D and LRRC8E (Fig. 3B). *LRRC8(B,C)*$^{-/-}$ cells displayed up to a twofold higher swelling-induced efflux compared to WT cells, suggesting that the genetic removal of LRRC8B and LRRC8C increases the abundance of organic compound-conducting LRRC8A/D, LRRC8A/E and probably LRRC8A/D/E channels. Conversely, disruption of both *LRRC8D* and *LRRC8E* almost abolished (*myo*-inositol) or strongly suppressed (D-aspartate and taurine) transport of these compounds (Fig. 3B).

We conclude that LRRC8B and LRRC8C are neither required nor sufficient (together with LRRC8A) for the transport of the tested compounds, the exception being aspartate and taurine that can also be transported, albeit less efficiently, by LRRC8A/C and, most likely, LRRC8A/B/C heteromers.

In conclusion, LRRC8D has a major role in the permeability of VRAC for all tested organic compounds and, when co-expressed with LRRC8A, suffices for their efficient transport. However, as already noticed previously for taurine (Planells-Cases et al., 2015), LRRC8D is not absolutely required for VRAC-dependent transport of organic substrates. LRRC8E stands out in transporting (together with LRRC8A) aspartate apparently as efficiently as LRRC8D (with minor effects on the other substrates), whereas LRRC8C also supports the transport of aspartate and taurine but less efficiently.

Apparent substrate selectivity of cells expressing different LRRC8 combinations

We next systematically determined the apparent selectivity of HEK293 cells engineered to express, in addition to LRRC8A, only one, two, or three other LRRC8 isoforms. Hypotonicity-induced

Journal of Cell Science (2017) 130, 1122-1133 doi:10.1242/jcs.196253

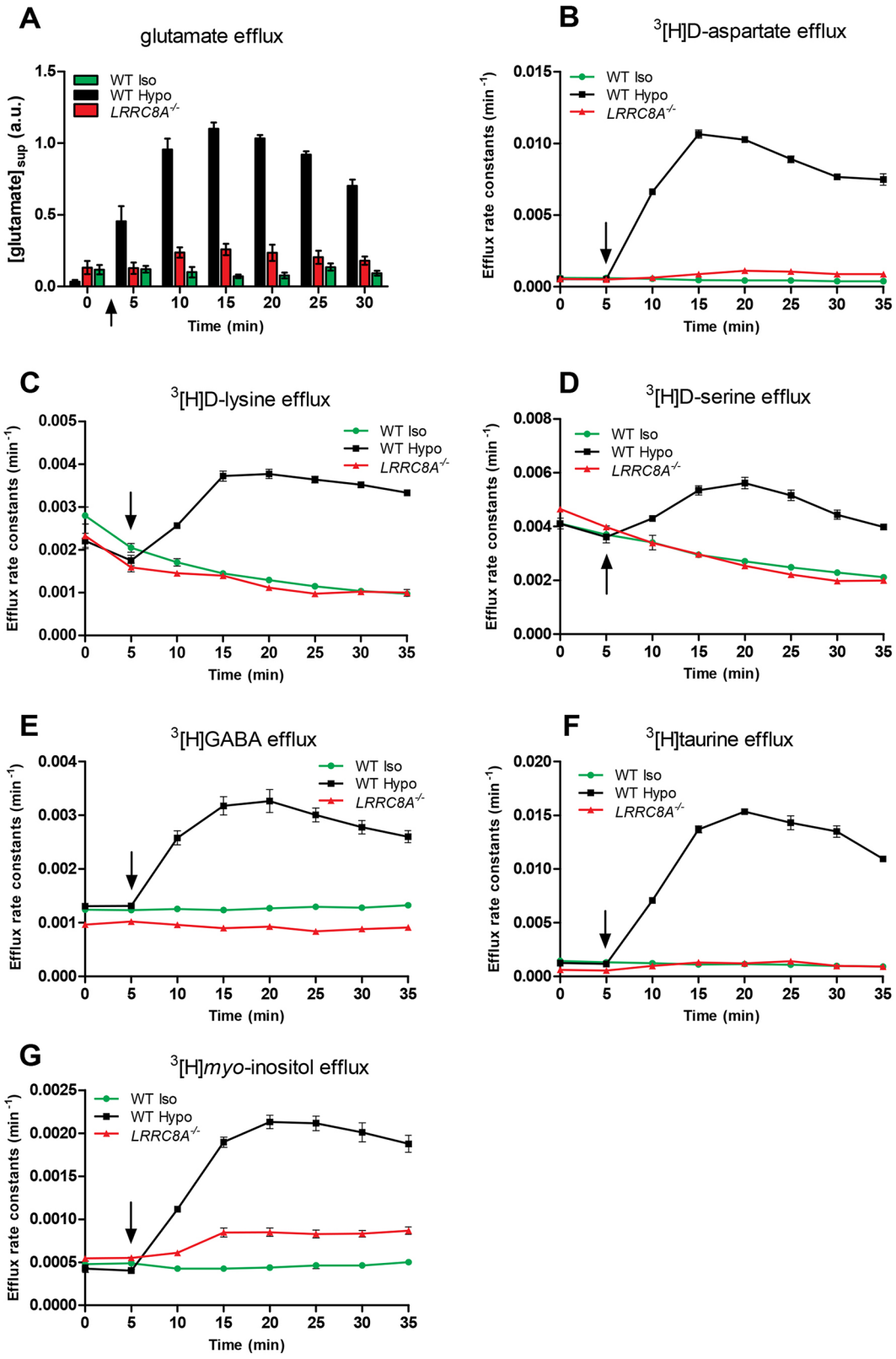

Fig. 1. Swelling-induced efflux of neurotransmitters and modulators from HEK293 cells depends on LRRC8A. (A) Efflux of cellular glutamate was measured by determining its levels in supernatant that was collected every 5 min. Cells were challenged with hypotonic solution at the time indicated by the arrow and glutamate concentrations in supernatants were determined using an enzymatic detection assay (a.u., arbitrary units). (B–F) Efflux rate constants of radiolabeled compounds from HEK293 cells that had been loaded with the indicated tracers. Radioactivity was measured in supernatants collected as in A. Efflux rate constants were determined as described in the Materials and Methods. Throughout mean±s.e.m values are given, with $n \geq 5$ (n denoting the number of wells tested). Note, error bars are often too small to be visible. Iso, efflux into isotonic (320 mOsm) medium; Hypo, efflux into hypotonic medium (240 mOsm).

Journal of Cell Science (2017) 130, 1122-1133 doi:10.1242/jcs.196253

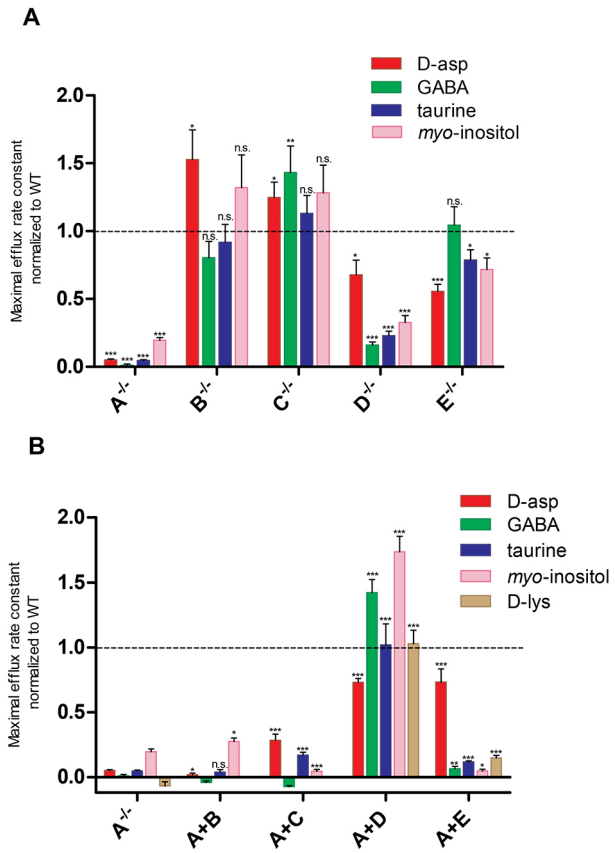

Fig. 2. Efflux of organic VRAC substrates as a function of LRRC8 isoforms. (A) Efflux of radiolabeled compounds in cells lacking one of the subunits LRRC8A to LRRC8E, and (B) triple knockout cells in which only LRRC8A together with either LRRC8B, LRRC8C, LRRC8D or LRRC8E are left intact. Taurine efflux data shown for '$D^{-/-}$', 'A+C', 'A+D', and 'A+E' have been published previously (Planells-Cases et al., 2015) and are depicted again for comparison. Maximal swelling-induced rate constants were calculated and normalized to respective WT values (indicated by dashed line). Values for LRRC8A were partially derived from experiments shown in Fig. 1. Mean±s.e.m. values of at least three (A) or two (B) independent experiments (n=16 for A; and n=8 for B). *P≤0.05; **P≤0.01; ***P≤0.001 [Mann–Whitney test compared with WT (A) or *LRRC8A*$^{-/-}$ (B) values].

efflux of D-aspartate, taurine and *myo*-inositol, as representing negatively charged, zwitterionic and uncharged substrates, respectively, was determined for each of these cell lines. To compare fluxes quantitatively, we minimized variations in experimental conditions by testing all three compounds on the same batch of cells in a single experiment. We compared fluxes within these single experiments by normalizing rate constants of fluxes of taurine and *myo*-inositol to those of aspartate (Fig. 4). It should be noted, however, that the measured transport ratios of radioactively labeled compounds only serve to determine the apparent selectivity of VRACs as a function of available LRRC8 subunits. These ratios do not reflect the relative total fluxes of compounds since we ignore the intracellular concentration of the corresponding unlabeled molecules. As discussed later, the ratios neither reflect the selectivity of individual VRAC channels (i.e. biophysical properties of defined LRRC8 heteromers) but rather the physiologically important averaged selectivity of the entire ensemble of differently composed heteromers expressed in these cells.

We compiled Fig. 4 to compare the effect of an 'addition' of a particular LRRC8 isoform to a cell expressing sets of other isoforms. For instance, we display in Fig. 4A,B the effect the additional expression of LRRC8B has on taurine:aspartate and *myo*-inositol:aspartate flux ratios in cells expressing already two, three or four LRRC8 isoforms in all possible combinations. The additional expression of LRRC8B markedly increased the taurine:aspartate transport ratios in cells expressing LRRC8D, the subunit that enhances taurine flux (Fig. 2), but lacking LRRC8E (Fig. 4A). However, the addition of LRRC8B had no consistent effect on the *myo*-inositol:aspartate transport ratio (Fig. 4B). The increase of the taurine:aspartate transport ratio upon addition of LRRC8B to cells expressing LRRC8A and LRRC8D cannot be explained by the expression of additional LRRC8A/B channels (which lack significant transport activity, Fig. 2B), but rather suggests the formation of VRACs that contain LRRC8A, LRRC8B and LRRC8D subunits in a single heteromeric channel.

Conversely, addition of LRRC8C decreased the ratio of taurine (Fig. 4C) or *myo*-inositol (Fig. 4D) to aspartate flux in cells expressing only LRRC8A and LRRC8D (and simultaneously lacking LRRC8E). This effect might be due to the formation of separate LRRC8A/C channels that conduct taurine or *myo*-inositol only poorly and compete with the formation of LRRC8A- and LRRC8D-containing channels. However, a more likely scenario is that insertion of LRRC8C into channels containing both LRRC8A and LRRC8D decreases their taurine or *myo*-inositol over aspartate transport ratio.

As expected from the crucial role of LRRC8D in taurine (Planells-Cases et al., 2015) and, to a lesser extent, in aspartate transport (Fig. 2), the 'addition' of LRRC8D increased the taurine:aspartate transport ratio when added to all possible combinations of LRRC8A with other isoforms (Fig. S2A). Conversely, the addition of LRRC8E, which supports aspartate but not taurine transport (Fig. 2), decreased the taurine:aspartate flux ratio of cells co-expressing LRRC8D (i.e. the only cells displaying substantial taurine transport) (Fig. S2C). Qualitatively similar effects of LRRC8D or LRRC8E 'addition' were observed for the relative flux of *myo*-inositol (Fig. S2B,D), which also depends on LRRC8D but not LRRC8E (Fig. 2). In a proof-of-principle experiment, we partially rescued the effect of *LRRC8E* disruption on apparent channel selectivity by transient expression of LRRC8E (Fig. S2E, F). Such rescue experiments are somewhat problematic as only a fraction of cells are transfected, and because the overexpression in those cells likely skews the channel assembly and may even lead to an overall decrease in transport activity (Voss et al., 2014).

Sequential co-immunoprecipitation confirms that individual VRACs can contain at least three different LRRC8 subunits

We sought to confirm the formation of VRACs containing more than two different LRRC8 isoforms, which is suggested by our flux measurements, by sequential co-immunoprecipitations. Different epitopes were added to the C-termini of LRRC8A and LRRC8C and these constructs were co-expressed, together with untagged LRRC8E, in different combinations in *LRRC8*$^{-/-}$ HEK293 cells (i.e. cells lacking all LRRC8 isoforms). In contrast to LRRC8B and LRRC8D, these subunits can be robustly overexpressed in transfected cells (Voss et al., 2014). Solubilized membrane proteins were sequentially precipitated with beads coated with nanobodies against epitopes fused to LRRC8A and LRRC8C and the final precipitate probed with antibodies against LRRC8E (Fig. 5). Negative controls included cells expressing untagged LRRC8A and LRRC8C and the mixture of solubilized proteins from cells expressing LRRC8A with either LRRC8C or LRRC8E. These experiments established the presence of VRACs containing all three LRRC8 subunits in the same complex (Fig. 5).

Journal of Cell Science (2017) 130, 1122-1133 doi:10.1242/jcs.196253

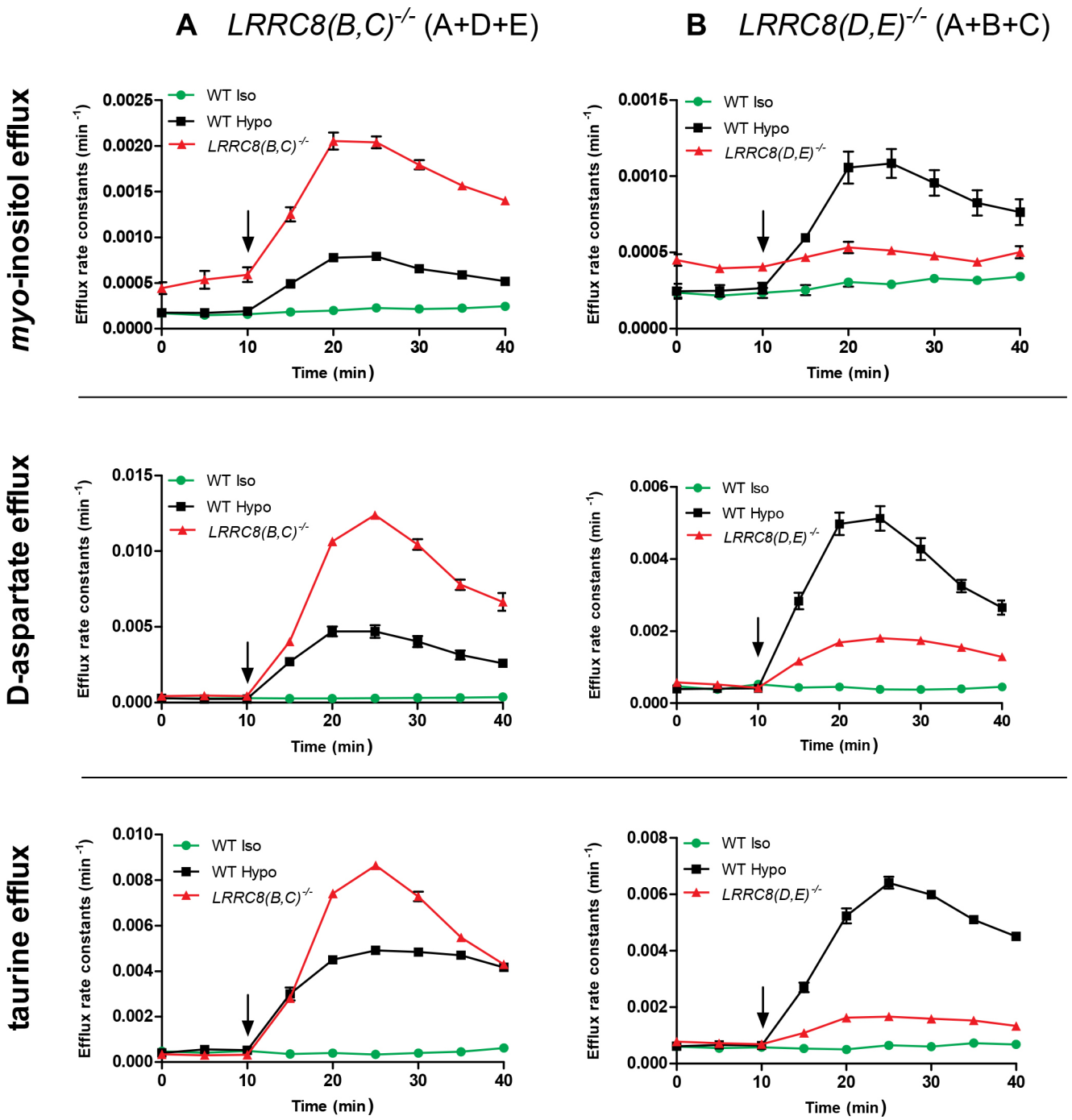

Fig. 3. LRRC8D and LRRC8E as crucial subunits for swelling-induced transport of organic substrates. Swelling-induced efflux rate constants of ^{3}[H]*myo*-inositol, ^{3}[H]D-aspartic acid and ^{3}[H]taurine in HEK293 cells either expressing VRAC heteromers containing subunits A+D+E [*LRRC8(B,C)*$^{-/-}$ cells; A], or subunits A+B+C [*LRRC8(D,E)*$^{-/-}$ cells; B] were determined as described in Fig. 2. *n*=4, error bars are s.e.m. Similar results were obtained in two independent experiments. Cells were challenged with hypotonic solution at the time indicated by the arrow.

Electrophysiological characterization of different VRAC heteromers

To compare fluxes of organic molecules to chloride currents, we analyzed the swelling-activated VRAC current $I_{Cl,vol}$ in all knockout cell lines by using the patch clamp technique. While single *LRRC8* gene disruptions affected inactivation kinetics as described for HCT116 cells (Voss et al., 2014) (Fig. 6A), all single knockout HEK293 cell lines (except *LRRC8A*$^{-/-}$ cells) still yielded robust swelling-activated currents that did not differ significantly from WT in magnitude or rectification (Fig. 6C). Similarly, double knockouts had only marginal effects on swelling-activated current densities with the exception of *LRRC8(C,E)*$^{-/-}$ cells, which showed a substantial reduction of currents (Fig. 6D). $I_{Cl,vol}$ rectification was increased in these cells, resembling currents reported for LRRC8A/D heteromers (Syeda et al., 2016). We hypothesize that currents in these cells are indeed mostly carried by LRRC8A/D channels, since the LRRC8A/B combination was found to yield only a very small $I_{Cl,vol}$ in overexpression or reconstitution

Journal of Cell Science (2017) 130, 1122-1133 doi:10.1242/jcs.196253

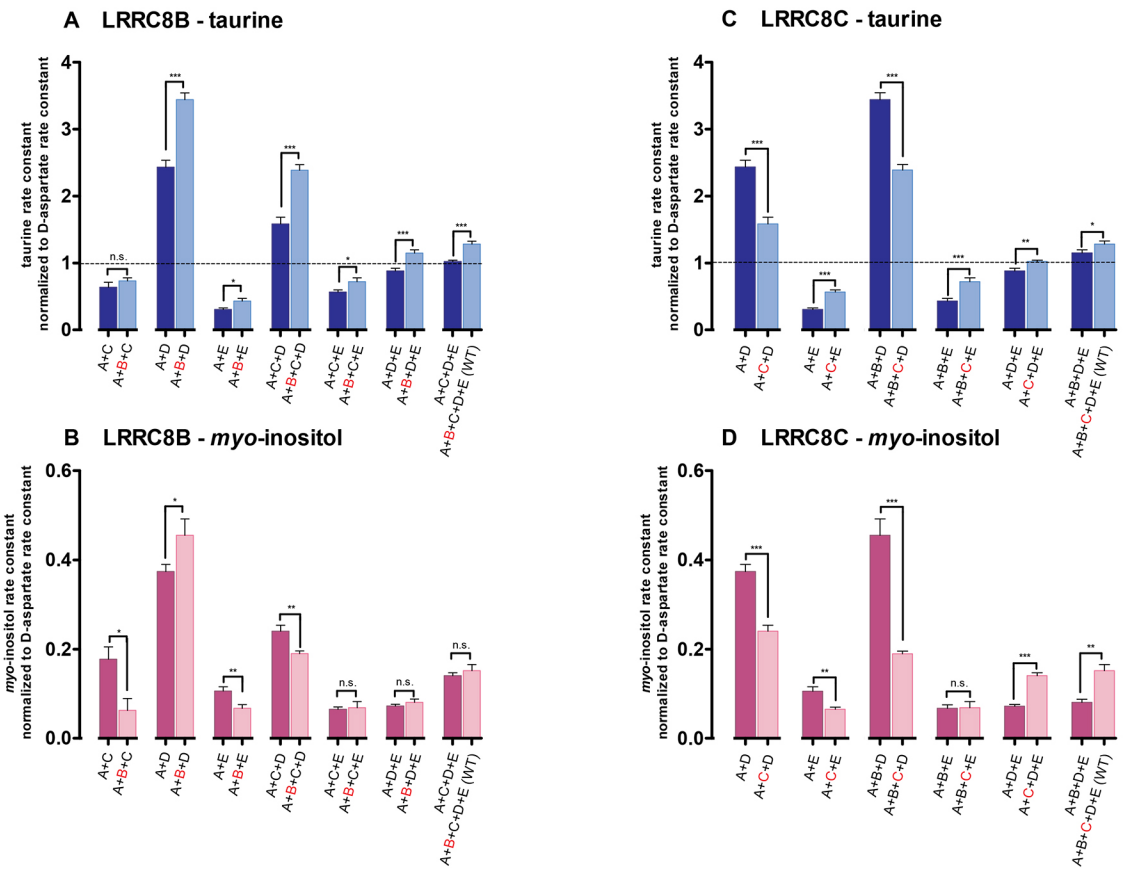

Fig. 4. Apparent substrate selectivity of differently composed VRAC heteromers. Influence of additional expression of LRRC8B (A,B) or LRRC8C (C,D) on the ratio of ^{3}[H]taurine (A,C) or ^{3}[H]*myo*-inositol (B,D) over ^{3}[H]D-aspartate transport. Values shown represent rate constants for taurine (A,C) or myo-inositol (B,D) (15 min after changing to hypotonic medium) normalized to rate constants for D-aspartate at the same time. Ratios of respective rate constants are depicted as bars that are grouped to easily compare HEK293 clones lacking (dark bars) or expressing (light bars) LRRC8B or LRRC8C, respectively. The dotted line in A and C reflects D-aspartate efflux rates but is cut off in B and D due to small values. Experiments used various knockout cell lines in which all LRRC8 subunits are expressed from endogenous promotors. Mean±s.e.m. values of two independent experiments (n=4 each for each substrate) are shown. *P≤0.05; **P≤0.01; ***P≤0.001 (Mann–Whitney test).

experiments (Syeda et al., 2016; Voss et al., 2014). Accordingly, no $I_{Cl,vol}$ could be evoked in *LRRC8(C,D,E)*$^{-/-}$ cells, in which only LRRC8A and LRRC8B are present (Fig. 6B,E). Cells only expressing LRRC8A/C or LRRC8A/E heteromers yielded substantial currents, which displayed the slow or fast inactivation gating already reported for these combinations, respectively (Fig. 6B,E; Voss et al., 2014). Reminiscent of our observations in *LRRC8(C,E)*$^{-/-}$ cells, LRRC8A/D-expressing cells showed a strongly reduced $I_{Cl,vol}$ with more pronounced outward rectification and intermediate inactivation gating (Fig. 6B,E).

We conclude that the $I_{Cl,vol}$ in HEK293 cells is probably carried by all LRRC8 isoforms. Whereas the LRRC8A/B combination was not able to support chloride currents in *LRRC8(C,D,E)*$^{-/-}$ HEK293 cells (Fig. 6B), small $I_{Cl,vol}$ currents were detected in HCT116 cells with the same *LRRC8* genotype (Voss et al., 2014), demonstrating that LRRC8B is indeed able to form functional VRACs with LRRC8A alone. LRRC8D, while pivotal for the transport of organic compounds, was able to produce an $I_{Cl,vol}$ in LRRC8A/D heteromers, albeit with strongly reduced current amplitudes (Planells-Cases et al., 2015) and changed inactivation kinetics (Fig. 6B). On the other hand, LRRC8A/C and LRRC8A/E supported WT-like $I_{Cl,vol}$, differing only in inactivation at strongly depolarized membrane potentials.

To assess electrogenic transport of organic substrates through VRACs, we measured swelling-activated currents after replacing a large part (105 mM) of the extracellular NaCl with NMDG-Cl, Na-aspartate, Na-glutamate, or taurine (the latter at pH 8.35 to obtain mainly negatively charged ions) (Fig. S3A,B). Surprisingly, we did not find significant differences in reversal potential shifts between wild-type VRACs and LRRC8A/C, LRRC8A/D, and LRRC8A/E heteromers for any of the tested compounds (Fig. S3A,B). The shift in reversal potentials upon partial external Cl^- replacement (Fig. S3A,B) was significantly different from the calculated shift in Cl^- reversal potential, indicating a contribution of currents carried by organic anions. To more sensitively test for such currents and their dependence on VRAC, we completely replaced external (but not internal) Cl^- by these compounds and compared currents at inside-positive voltages between HEK293 cells displaying different *LRRC8* genotypes (Fig. S3C,D). Whereas outward currents carried by Cl^- influx were clearly different between the different genotypes (and almost absent in *LRRC8*$^{-/-}$ cells, as expected), organic anion-mediated outward currents (i.e. organic anion influx) were independent of LRRC8 proteins as they displayed similar amplitudes in *LRRC8*$^{-/-}$ cells. This suggests the presence of a VRAC-independent electrogenic uptake of organic anions at strongly positive potentials. The VRAC-(LRRC8-)dependent transport of organic compounds that we have established by flux measurements cannot be detected by electrophysiological methods in HEK293 cells because of background problems.

Journal of Cell Science (2017) 130, 1122-1133 doi:10.1242/jcs.196253

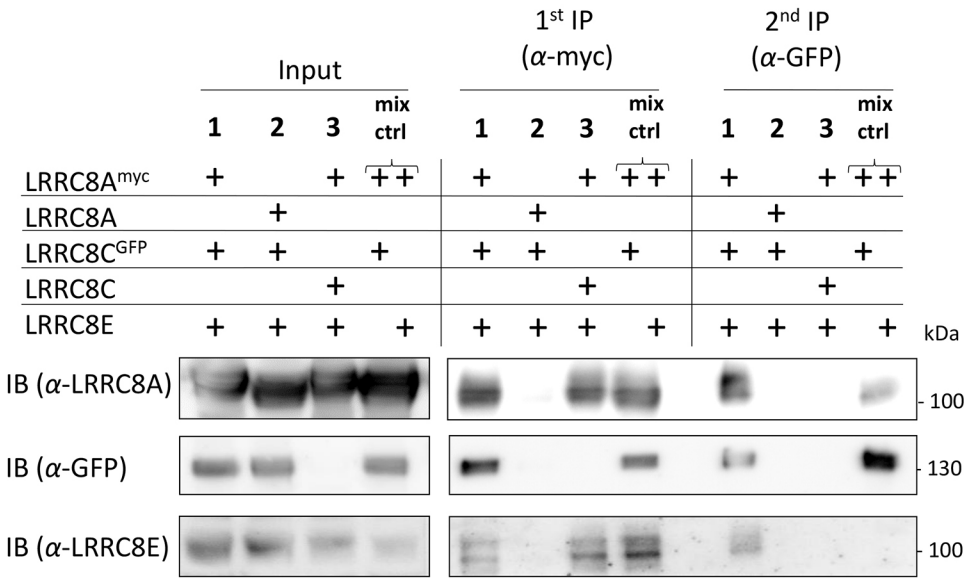

Fig. 5. Sequential co-immunoprecipitation of VRAC heteromers. Sequential co-immunoprecipitation (IP) of LRRC8 heteromers with antibodies against LRRC8A and LRRC8C, respectively, and probing for LRRC8E reveals the presence of heteromers containing all three subunits. HEK293 *LRRC8*$^{-/-}$ cells lacking all five LRRC8 isoforms were transfected with Myc-tagged LRRC8A (LRRC8A^{myc}), GFP-tagged LRRC8C (LRRC8C^{GFP}) and untagged LRRC8E. Solubilized proteins were sequentially affinity-purified with anti-Myc and anti-GFP antibodies. Controls include untagged LRRC8A or LRRC8C (fractions 2 and 3, respectively). In the 'mix control', HEK293 *LRRC8*$^{-/-}$ cells were transfected either with LRRC8A^{myc} and LRRC8C^{GFP}, or LRRC8A^{myc} and LRRC8E, respectively, and cell lysates pooled prior to the first affinity purification to control for *in vitro* aggregation of A/C and A/E VRAC heteromers.

DISCUSSION

Over the past decades many organic compounds have been suggested to be transported by VRAC or other volume-regulated osmolyte or anion channels, but the unknown identity of the proteins forming VRACs precluded rigorous conclusions. We have now demonstrated that several chemically distinct organic compounds permeate LRRC8 (VRAC) channels and discovered a special role of LRRC8D and LRRC8E subunits in the transport of all tested organic compounds, and of electrically negatively charged aspartate and glutamate, respectively. Our work reveals that several neurotransmitters and co-activators pass through VRACs, including the main inhibitory neurotransmitter GABA, which had not been previously recognized as VRAC substrate. This suggests that differently composed VRACs may play important modulatory roles in the signal transduction in the nervous system.

VRACs as major osmotically-induced pathway for various organic compounds

LRRC8A is the only obligatory VRAC subunit (Qiu et al., 2014; Voss et al., 2014). It forms functional channels with any of the four other LRRC8 isoforms and is needed for their transport to the plasma membrane (Voss et al., 2014). Disruption of *LRRC8A* using CRISPR/Cas9 genomic editing provides an easy and stringent test for the involvement of VRAC in defined transport processes (Voss et al., 2014). It gives more clear-cut results than siRNA knockdown (Hyzinski-García et al., 2014; Qiu et al., 2014) and is by far superior to pharmacological studies as there are no specific VRAC inhibitors. Of note, several VRAC inhibitors also block pannexins, connexins and glutamate transporters (Abdullaev et al., 2006; Benfenati et al., 2009; Bowens et al., 2013; Ye et al., 2009), all of which are candidate proteins for the release of amino acids.

Disruption of *LRRC8A* abolished the bulk of hypotonicity-activated cellular efflux of L-glutamate, D-aspartate, D-lysine, D-serine, GABA, taurine and *myo*-inositol (Fig. 1), identifying VRACs as the major swelling-activated efflux pathway for these compounds in HEK293 cells. Together with platinum-based drugs (Planells-Cases et al., 2015) and blasticidin S (Lee et al., 2014), we now have a large list of confirmed organic substrates of LRRC8 channels. The diverse physicochemical properties of organic VRAC substrates suggest a rather wide and poorly specific permeation pathway. A poorly selective pore that conducts structurally dissimilar and differently charged organic compounds seems to contrast with the ability of VRACs to strongly discriminate between inorganic anions and cations and mildly even between iodide and chloride ions (Gosling et al., 1995; Kubo and Okada, 1992; Nilius et al., 1997; Pedersen et al., 2016). This apparent discrepancy may now be partially explained by the presence of different LRRC8 heteromers with different pore properties.

VRAC versus VSOAC

For a long time, it has remained unclear whether 'VRAC', the volume-regulated anion channel, is distinct from 'VSOAC' (Jackson et al., 1994), the volume-sensitive organic osmolyte/anion channel (Shennan, 2008). Transport of both halides and organic osmolytes (e.g. taurine) was stimulated by cell swelling and could be inhibited by an overlapping spectrum of (non-specific) inhibitors. However, halide and organic osmolyte efflux increased with different timecourses after exposure to hypotonicity and their sensitivity to drugs differed in detail, leading to the proposal that 'VRAC' is different from 'VSOAC' (Lambert and Hoffmann, 1994; Shennan, 2008; Stutzin et al., 1999). This hypothesis was further supported by the conceptual difficulty of imagining channel pores transporting comparatively large organic compounds while displaying pronounced anion selectivity with small inorganic ions.

The discovery that LRRC8A is indispensable for both swelling-activated Cl^- currents and taurine fluxes (Qiu et al., 2014; Voss et al., 2014) was compatible with VRAC being identical to VSOAC. However, cells may express different LRRC8 heteromers that differ in inactivation kinetics (Voss et al., 2014) and substrate selectivity (Planells-Cases et al., 2015; Syeda et al., 2016). Taurine transport

Journal of Cell Science (2017) 130, 1122-1133 doi:10.1242/jcs.196253

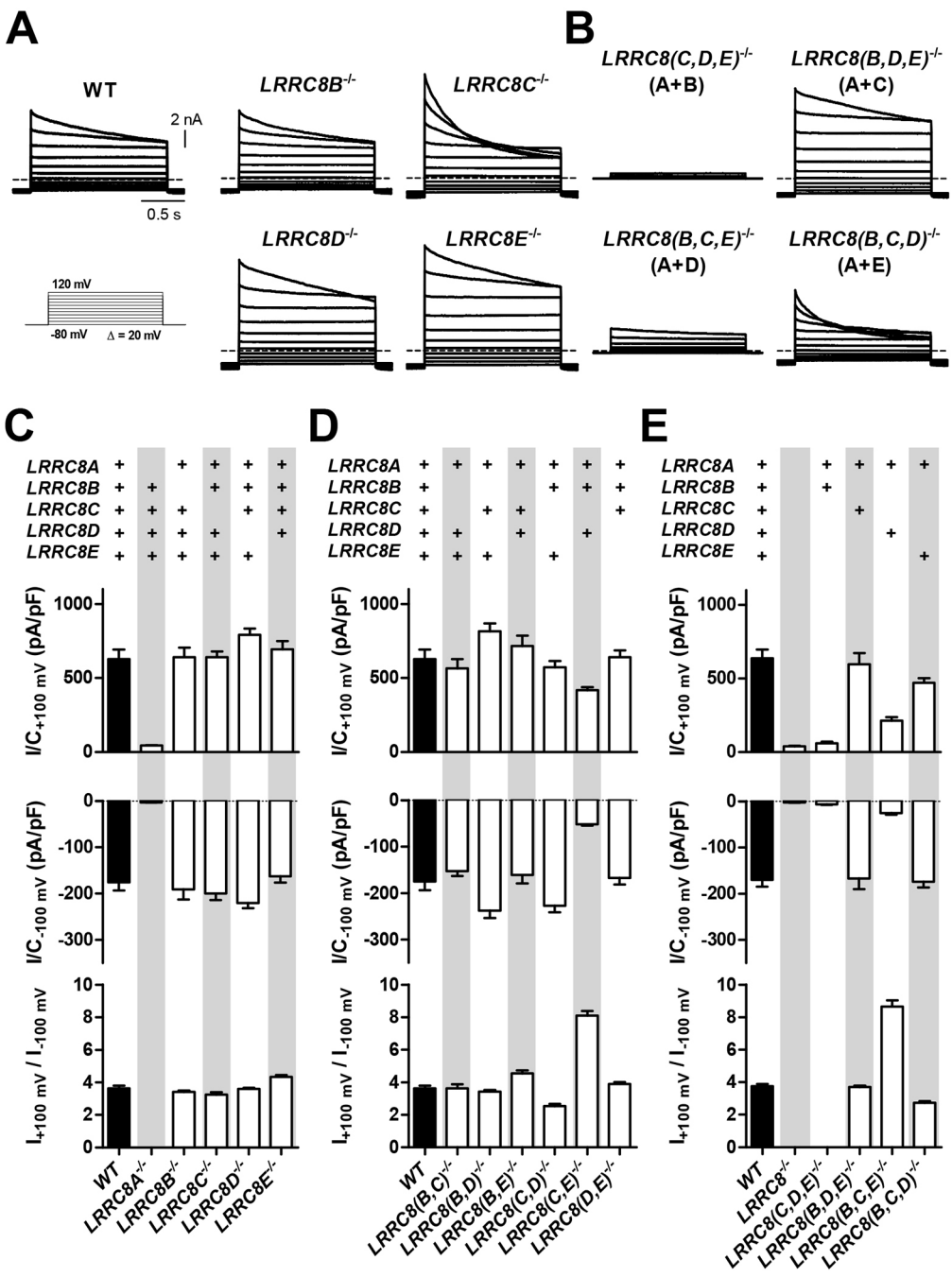

Fig. 6. Electrophysiological characterization of VRAC currents in HEK293 cells expressing different LRRC8 combinations. (A,B) Representative VRAC current ($I_{Cl,vol}$) traces in response to the voltage clamp protocol shown in (A) applied to cells in which one (A) or three (B) LRRC8 isoforms were genetically disrupted. Dashed lines indicate zero current. (C,D,E) $I_{Cl,vol}$ current densities at +100 mV (top) or –100 mV (middle), and the rectification coefficient (bottom) of the indicated LRRC8 single- (C), double- (D), or triple-knockout cell lines (E). Error bars are s.e.m. All experiments were repeated in 8–12 independent cells on at least three different days.

through VRAC depends very strongly, though not absolutely (Fig. 3B ; Planells-Cases et al., 2015), on the presence of LRRC8D, as does the transport of blasticidin S (Lee et al., 2014) and of the anti-cancer drugs cisplatin and carboplatin (Planells-Cases et al., 2015). We now showed that LRRC8D also has a pivotal role for the transport of aspartate, lysine, GABA and *myo*-inositol (Fig. 2A,B). However, LRRC8D is not the only VRAC subunit supporting the transport of organic compounds. This is particularly evident for aspartate, which was transported by LRRC8A/D- or LRRC8A/E-expressing cells with similar efficacies, and which could also pass through LRRC8A/C (Fig. 2B) and LRRC8A/B/C (Fig. 3B) channels. Hence organic compound-transporting 'VSOACs' cannot be discriminated from halide ion-transporting 'VRACs' by the presence of LRRC8D or LRRC8E. Of note, LRRC8A/E, LRRC8A/C and (to a lesser degree) LRRC8A/D heteromers also yield Cl^- currents (Fig. 6). While this suggests that there is no separation into exclusively halide- or organic compound-selective pores, we cannot exclude the possibility that, for instance, LRRC8A and LRRC8D can assemble to hexamers with different stoichiometries, resulting in two classes of channels that transport exclusively either halides or organic compounds. Although LRRC8D-containing VRACs are more 'VSOAC-like', a strict conceptual separation into VRAC and VSOAC channels does not seem warranted.

LRRC8D and LRRC8E in the transport of neutral and negatively charged organic compounds

Whereas LRRC8D, together with LRRC8A, supported the transport of all tested organic compounds, LRRC8E rather specifically supported the transport of the negatively charged aspartate. Since swelling-induced Cl^- currents were also larger with LRRC8A/E

Journal of Cell Science (2017) 130, 1122-1133 doi:10.1242/jcs.196253

than with LRRC8A/D channels (Fig. 6), we hypothesize that LRRC8E enhances the transport of negatively charged ions. In contrast, LRRC8D allows the transport of organic compounds irrespective of charge, that is, negatively charged aspartate, electrically neutral molecules [either uncharged like *myo*-inositol or zwitterionic (such as taurine, serine, and GABA at physiological pH)], partially positively charged compounds such as cisplatin (Planells-Cases et al., 2015) and blasticidin S (Lee et al., 2014), and even almost fully positively charged lysine.

Disruption of LRRC8B or LRRC8C did not decrease the transport of organic compounds (Fig. 2A). *LRRC8(C,D,E)*$^{-/-}$ HEK293 cells expressing only LRRC8A/B virtually lacked both transport of organic compounds and $I_{Cl,vol}$ (Figs 2B and 6). However, *LRRC8(C,D,E)*$^{-/-}$ HCT116 cells do yield VRAC currents (Voss et al., 2014), suggesting that HEK293 cells might express very few LRRC8A/B channels, precluding conclusions on their ability to transport organic substrates. LRRC8A/C channels, on the other hand, were clearly able to support aspartate flux, but mediated only small or insignificant transport of taurine (Planells-Cases et al., 2015), GABA and *myo*-inositol (Fig. 2B).

Complexity of LRRC8 heteromers

Based on the homology of LRRC8 proteins to pannexins (Abascal and Zardoya, 2012), VRACs are believed to assemble into hexamers (Syeda et al., 2016; Voss et al., 2014). The obligatory subunit LRRC8A can bind to any of the other LRRC8 proteins as demonstrated by functional assays (Planells-Cases et al., 2015; Voss et al., 2014) and co-immunoprecipitation (Lee et al., 2014; Syeda et al., 2016; Voss et al., 2014). As most WT cells probably express four to five *LRRC8* genes, albeit to different degrees (Voss et al., 2014), individual cells may express a large variety of different VRAC channels. These contain at least two and possibly up to five different LRRC8 subunits within an individual channel. Our experiments therefore reflect average transport properties of an ensemble of different channels. This may even be true when cells express only two different LRRC8 proteins, because they might assemble with different stoichiometries. So far, we have no clue on these stoichiometries.

Our functional assays (Fig. 4A) and sequential co-immunoprecipitations (Fig. 5) now revealed that individual VRACs may contain more than two LRRC8 subunits. Under the assumption that all subunits can assemble with identical affinities and that VRACs are hexamers, cells expressing three or more different LRRC8 subunits to about the same level will contain only minute amounts of VRACs composed of only two different LRRC8 isoforms. Although we cannot assign the transport activities assessed here to single, defined heteromeric channels, our work has revealed the contributions of particular LRRC8 isoforms to the transport of different substrates.

We also tried to electrophysiologically characterize the transport of organic compounds by diverse LRRC8 heteromers by measuring reversal potentials with aspartate, glutamate or taurine as charge carriers. Whereas native VRACs have been suggested to yield currents with organic anions (Banderali and Roy, 1992; Boese et al., 1996; Jackson and Strange, 1993; Manolopoulos et al., 1997), this notion could not be rigorously tested previously owing to the lack of genetic and specific pharmacological tools. We now showed that, at least in HEK293 cells, organic anion-mediated currents at positive voltages are almost totally independent of VRAC. Hence, previous reports on organic anion-mediated currents through VRAC should be viewed with caution. Indeed, a pioneering study by Banderali and Roy (1992) used Ca^{2+}- and ATP-free intracellular solutions, which preclude the activation of VRACs (Jackson et al., 1994; Nilius et al., 1997). The LRRC8-independent organic anion current identified here was only observed at non-physiological, positive voltages. Hence, it does not interfere with the VRAC-dependent transport of neurotransmitters and other compounds, which we studied using radiotracer fluxes at physiological potentials.

A recent report on LRRC8 channels heterologously expressed in *Xenopus* oocytes (Gaitán-Peñas et al., 2016) did not reveal significant differences in reversal potentials for several organic compounds (including glutamate, aspartate and lactate) between different LRRC8 heteromers, with the exception of taurine and glycine that seemed to better permeate LRRC8A/D than LRRC8A/C or LRRC8A/E channels. The reason for the apparent discrepancy to our work is unclear, but might be related to differences in background currents between *Xenopus* oocytes and HEK293 cells. Unlike our *LRRC8*$^{-/-}$ HEK293 cells, oocytes endogenously express LRRC8 proteins, which might heteromerize with heterologously expressed subunits and confound results. The same report (Gaitán-Peñas et al., 2016) failed to detect differences between differently composed LRRC8 channels in fluxing organic compounds due to a saturation of uptake in their experiments (Gaitán-Peñas et al., 2016), in stark contrast to our work which revealed highly relevant differences between diverse VRACs to transport organic compounds.

VRACs in the release of neurotransmitters

Our experiments showed that LRRC8 heteromers (VRACs) can transport several neurotransmitters and modulators, including the main excitatory and inhibitory neurotransmitters glutamate and GABA, respectively, as well as the co-activator D-serine and the glycine receptor agonist taurine. In the brain, the role of VRAC in releasing neurotransmitters and modulators may be similarly important to its function in cell volume regulation, or even more so. Both neurons and astrocytes express VRACs (Akita and Okada, 2014), and contain the neurotransmitters and co-agonists studied here. Astrocytes take up extracellular glutamate and GABA through ion-coupled transporters to remove them from the extracellular space after their exocytosis at synapses. Moreover, astrocytes not only synthesize glutamate, but also GABA (Yoon et al., 2014) and D-serine (Wolosker et al., 1999). VRAC-mediated neurotransmitter release may be more prominent with astrocytes than with neurons because they are more prone to swell, at least under hypoxic conditions (Mongin, 2015). On the other hand, axons swell slightly upon action potential firing (Fields and Ni, 2010; Iwasa et al., 1980; Kim et al., 2007) and may release ATP through swelling-activated anion channels (Fields and Ni, 2010). A role of VRACs in neurotransmitter release from neurons, however, remains speculative.

By contrast, it is well established that astrocytes are capable of releasing transmitters like glutamate, aspartate, D-serine, taurine and ATP (Harada et al., 2015; Kimelberg et al., 1990; Parpura et al., 1994; Pasantes-Morales et al., 1994). It has been suggested that this ‘gliotransmitter’ release influences neuronal excitability, adding a novel component to neuronal information processing (Verkhratsky et al., 2016, 2012). The mechanisms by which astrocytes release neurotransmitters include vesicle exocytosis, reversal of transporters that normally remove neurotransmitters from the extracellular space and channel-like processes (Hamilton and Attwell, 2010; Montero and Orellana, 2015). Whereas VRAC/VSOAC has been implicated in the swelling-activated release of taurine, glutamate, aspartate and D-serine (Rosenberg et al., 2010), its ability to release ATP is debated (Burow et al., 2015; Hazama

Journal of Cell Science (2017) 130, 1122-1133 doi:10.1242/jcs.196253

et al., 1999; Hisadome et al., 2002) and might occur only at extreme levels of hypotonic swelling (Gaitán-Peñas et al., 2016). Another, molecularly unidentified maxi-anion channel may rather mediate swelling-induced ATP release (Sabirov et al., 2016).

Two potential roles of VRACs in brain physiology and pathology have received particular attention. VRACs may play a role in systemic volume regulation by releasing taurine from swollen astrocytes in the supraoptical nucleus. Taurine then activates inhibitory glycine receptors on somata of adjacent osmosensing neurons, which are themselves excited by hypertonic shrinkage and secrete water-retaining vasopressin in the pituitary (Hussy et al., 2000; Jentsch, 2016; Prager-Khoutorsky and Bourque, 2015; Prager-Khoutorsky et al., 2014). In stroke, hypoxic swelling of astrocytes may open VRACs that release glutamate, which in turn activates neuronal glutamate receptors (Akita and Okada, 2014; Inoue and Okada, 2007; Jentsch, 2016) and thereby increases infarct size through 'excitotoxicity' (Inoue et al., 2007; Mongin, 2015; Zhang et al., 2008). Interestingly, the brain almost lacks expression of LRRC8E (Voss et al., 2014), a subunit shown here to enhance aspartate (glutamate) efflux. Although LRRC8D-containing VRACs also transport glutamate, the low brain expression of LRRC8E may serve to minimize deleterious effects of this excitatory neurotransmitter during volume regulation or other processes that require VRAC opening. VRACs may also be activated without an increase of cell volume by several signaling molecules (Akita and Okada, 2011; Burow et al., 2015; Hyzinski-García et al., 2014; Mongin and Kimelberg, 2002) and in the course of apoptosis (Planells-Cases et al., 2015). If VRACs display low basal transport activity (Planells-Cases et al., 2015), they might also contribute to ambient (extracellular, extrasynaptic) GABA that has been controversially attributed to a bestrophin-mediated release from astrocytes (Diaz et al., 2011; Lee et al., 2010).

Hence, VRACs may be important players in modulating brain function in physiology and pathology. The identification of individual LRRC8 subunits in the transport of particular neuroactive molecules now allows us to investigate these roles using subunit- and cell-specific knockout mouse models. For instance, *Lrrc8d*$^{-/-}$ mice will be useful to assess the biological role of VRAC-dependent transport of taurine, inositol and GABA, while *Lrrc8(b,c)*$^{-/-}$ mice may help to elucidate effects of overall increased transport of organic compounds by VRAC. Moreover, the development of drugs specifically inhibiting VRACs containing particular LRRC8 subunit combinations, which seems possible (Planells-Cases et al., 2015), may offer novel therapeutic opportunities by inhibiting the transport of only a subset of VRAC substrates.

MATERIALS AND METHODS

If not stated otherwise, all experiments were performed at room temperature.

Measurement of swelling-induced efflux of endogenous glutamate

Wild-type and *LRRC8A*$^{-/-}$ HEK293 cells were grown on poly-L-lysine-coated (Sigma) six-well plates (Sarstedt) with Dulbecco's modified Eagle's medium (DMEM), fetal calf serum (FCS) and penicillin-streptomycin (Pan Biotech) to 70–80% confluency. Cell culture medium was aspirated and wells were washed 9× with 1 ml isotonic solution (in mM: 150 NaCl, 6 KCl, 1 $MgCl_2$, 1.5 $CaCl_2$, 10 glucose, 10 HEPES pH 7.4; 320±5 mOsm). The final wash was collected and put on ice for later analysis. Cells were then challenged with hypotonic solution (in mM: 105 NaCl, 6 KCl, 1 $MgCl_2$, 1.5 $CaCl_2$, 10 glucose, 10 HEPES pH 7.4, 240±5 mOsm) or isotonic solution as control. Solution was exchanged every 5 min (30 min in total) with fresh isotonic or hypotonic solution and supernatants were kept on ice. Samples were then centrifuged at 27 ***g*** to remove cellular debris. 50 µl of the supernatant were analyzed for glutamate content using the Amplex® Red Glutamic Acid/Glutamate Oxidase Assay Kit (Life Technologies) according to the manufacturer's manual.

Efflux assays using radioactively labeled tracers

Efflux assays were performed as described previously (Planells-Cases et al., 2015; Voss et al., 2014). HEK293 cells on poly-L-lysine-coated six-well plates (~70–80% confluent) were loaded with 2 µCi/ml ^{3}[H]γ-aminobutyric acid (Perkin Elmer), ^{3}[H]D-aspartic acid, ^{3}[H]D-serine, ^{3}[H]*myo*-inositol, ^{3}[H]D-lysine and ^{3}[H]taurine (Hartmann Analytics) for 2 h (^{3}[H]GABA, 60 min; ^{3}[H]*myo*-inositol, overnight). HEK293 cells used for ^{3}[H]GABA efflux were preincubated for 24 h with 100 µM vigabatrin (Sigma-Aldrich) to irreversibly inhibit intracellular GABA catabolism via GABA-transaminase. We used HEK293 rather than HCT116 cells (Voss et al., 2014) because they showed higher flux rates, which resulted in larger hypotonic:isotonic flux ratios.

After washing, cells were incubated with isotonic solution for 20 min. During this time, isotonic solution was exchanged every 5 min and kept for later analysis. Cells were then challenged with hypotonic solution (control, isotonic solution; both solutions as specified for glutamate efflux) for 30 min (exchange of solution every 5 min, all fractions collected for analysis). Finally, cells were lysed with 0.75 ml 0.1 M NaOH. Lysate was neutralized with 0.75 ml 0.1 M HCl. All fractions and lysates were analyzed for radioactivity by scintillation counting with 10 ml of the scintillation cocktail Aquasafe 300 plus (Zinsser Analytics) in a Tri-Carb 2810 TR β-scintillation counter (Perkin Elmer). Rate constants (min^{-1}) were calculated as described previously (Qiu et al., 2014). Rate constants of the final isotonic measurement were subtracted from rate constants obtained under hypotonicity to obtain swelling-induced rate constants. The maximal rate constants obtained were normalized to those of WT cells within the same experiment.

Possibly owing to different cell densities or other slight variations in experimental conditions, absolute flux rates for a given substrate and LRRC8 combination varied between experiments. To compare flux rates of different substrates for a particular LRRC8 combination, we therefore measured fluxes of three different substrates with the same cell line in a single experiment. This yielded well reproducible values for the flux ratios for different substrates. Fig. 4 and Fig. S2 depict the ratio of taurine or *myo*-inositol fluxes over those of D-aspartate, always measured at 15 min (when the efflux rate constant is close to maximum). For the *LRRC8E*$^{-/-}$ rescue experiment, cells were seeded on six-well plates and transiently transfected with an LRRC8E–GFP construct using Fugene®HD transfection reagent (Promega) 24 h prior to efflux measurements.

Generation of HEK293 cell lines with *LRRC8* gene disruptions using CRISPR/Cas9 technology

CRISPR/Cas9-mediated disruption of *LRRC8* genes in HEK293 cells was performed as described previously (Voss et al., 2014). In brief, target single guide (sg)RNAs (see Table S2) were cloned into a pX330 vector and transfected into HEK293 cells together (at a 9:1 ratio) with a plasmid used to express EGFP (pEGFP-C1). Two days after transfection, individual fluorescent cells were FACS-sorted into 96-well plates containing 80 µl preconditioned cell culture medium per well. Resulting monoclonal cell lines were tested for sequence alterations by sequencing of site-specific PCR amplicons. Only clones with frameshift mutations (except for clone 3E7, which has a 21 nucleotide deletion in transmembrane domain 1, see Table S1) were chosen and gene disruption was confirmed by western blotting (see Fig. S4) using antibodies described previously (Planells-Cases et al., 2015). To disrupt multiple *LRRC8* genes, respective sgRNAs (see Tables S1,S2 for a list of target sequences) were transfected together, or cell lines already carrying disrupted *LRRC8* genes were used for a new round of gene disruption.

Electrophysiology

The whole-cell patch clamp method was used to measure $I_{Cl,vol}$ as described previously (Planells-Cases et al., 2015; Voss et al., 2014). The pipette solution contained (in mM): 40 CsCl, 100 Cs-methanesulfonate, 1 $MgCl_2$, 1.9 $CaCl_2$, 5 EGTA, 4 Na_2ATP, and 10 HEPES, pH 7.2 with CsOH (290

mOsm). The hypotonic saline used to elicit $I_{Cl,vol}$ contained (in mM): 105 NaCl, 6 CsCl, 1 $MgCl_2$, 1.5 $CaCl_2$, 10 glucose, 10 HEPES, pH 7.4 with NaOH (240 mOsm). To measure reversal potential shifts, NaCl in the hypotonic saline was replaced with equimolar amounts of Na-aspartate or Na-glutamate, or with 210 mM taurine (pH 8.35 with NaOH).

For recordings of currents mediated exclusively by organic anions, the control solution contained (in mM): 114 NaCl, 6 HCl, 6 CsOH, 1 Mg-gluconate$_2$, 1.5 $Ca(OH)_2$, 10 HEPES, pH 7.4 with NaOH (240 mOsm). NaCl and HCl were replaced with equimolar amounts of Na-aspartate or Na-glutamate, and aspartic acid or glutamic acid, respectively. The taurine solution contained 228 mM taurine instead of NaCl and HCl (pH 8.35 with NaOH, adjusted to 240 mOsm with mannitol).

Cells were held at −30 mV and a 2.6-s ramp protocol from −100 mV to 100 mV was applied every 15 s to monitor $I_{Cl,vol}$ current densities developing over time. Maximally activated $I_{Cl,vol}$ was further characterized by 2-s step protocols from −80 mV to 120 mV in 20 mV increments, preceded and followed by 0.5-s steps to −80 mV to ensure full recovery from inactivation. Reversal potentials were measured using 2-s ramps from −80 mV to 80 mV preceded by 0.5-s steps to −80 mV.

Sequential co-immunoprecipitation

LRRC8$^{-/-}$ HEK293 cells lacking all five VRAC subunits were transiently transfected (using polyethylenimine, Polysciences) with expression constructs encoding Myc- or untagged LRRC8A, EGFP- or untagged LRRC8C, and untagged LRRC8E (epitopes were fused to C-termini). At 24 h post transfection (from here on, all steps were performed at 4°C unless stated otherwise), cells were collected and lysed in buffer containing 1% n-dodecyl-β-maltoside (DDM, Glycon), 150 mM NaCl, 50 mM Tris-HCl pH 7.5, 4 mM Pefabloc (Roth) and complete protease inhibitor cocktail (Roche). In 'mix controls' (Fig. 5), lysates from differently transfected cells were pooled. The lysate was cleared by centrifugation at ∼100,000 ***g*** for 45 min and incubated for at least 2 h with Myc-Trap®_MA beads (Chromotek). After washing, proteins were eluted with Myc peptide (Chromotek) and used for further precipitation using GFP-Trap® MA beads (Chromotek). After three additional washes with 1 ml lysis buffer, precipitates were eluted in 2× Laemmli sample buffer for 10 min at 75°C. Finally, proteins were separated by SDS-PAGE and analyzed by western blotting as indicated [using antibodies against LRRC8A and LRRC8E described previously (Planells-Cases et al., 2015) and ch@GFP (Aves Labs) for GFP detection]. Lysate equivalent to 25% and 1.6% of input for the first and second immunoprecipitation, respectively, and eluate of the first immunoprecipitation were loaded as reference.

Statistical analysis

Data are depicted as mean±s.e.m. (with *n* denoting the number of samples as indicated in respective figure legends). To compare groups of values (as shown in Figs 2 and 4 and Fig. S2), the Mann–Whitney test was employed, where significance was considered as follows: $*P \leq 0.05$; $**P \leq 0.01$; and $***P \leq 0.001$.

Acknowledgements

We thank Karolin Fuchs for technical assistance and Dr Jens Furkert for his patient and competent support in handling the radioisotope experiments.

Competing interests

The authors declare no competing or financial interests.

Author contributions

D.L. planned, performed and analyzed experiments (CRISPR/Cas9 mediated LRRC8 gene disruption, efflux measurements with radiolabeled isotopes) and wrote the paper; F.U. performed and analyzed electrophysiological experiments; J.C.L. planned, performed and analyzed Co-IP experiments; S.K. planned and analyzed preliminary measurements using gas chromatography–mass spectrometry; T.J.J. planned and analyzed experiments and wrote the paper.

Funding

This work was supported by a European Research Council Advanced Grant (FP/2007-2013) 294435 'Cytovolion' and the Deutsche Forschungsgemeinschaft (JE 164/12-1 and Exc257 'Neurocure') to T.J.J.

Supplementary information

Supplementary information available online at
http://jcs.biologists.org/lookup/doi/10.1242/jcs.196253.supplemental

References

Abascal, F. and Zardoya, R. (2012). LRRC8 proteins share a common ancestor with pannexins, and may form hexameric channels involved in cell-cell communication. *BioEssays* **34**, 551-560.

Abdullaev, I. F., Rudkouskaya, A., Schools, G. P., Kimelberg, H. K. and Mongin, A. A. (2006). Pharmacological comparison of swelling-activated excitatory amino acid release and Cl^- currents in cultured rat astrocytes. *J. Physiol.* **572**, 677-689.

Akita, T. and Okada, Y. (2011). Regulation of bradykinin-induced activation of volume-sensitive outwardly rectifying anion channels by Ca^{2+} nanodomains in mouse astrocytes. *J. Physiol.* **589**, 3909-3927.

Akita, T. and Okada, Y. (2014). Characteristics and roles of the volume-sensitive outwardly rectifying (VSOR) anion channel in the central nervous system. *Neuroscience* **275C**, 211-231.

Banderali, U. and Roy, G. (1992). Anion channels for amino acids in MDCK cells. *Am. J. Physiol.* **263**, C1200-C1207.

Benfenati, V., Caprini, M., Nicchia, G. P., Rossi, A., Dovizio, M., Cervetto, C., Nobile, M. and Ferroni, S. (2009). Carbenoxolone inhibits volume-regulated anion conductance in cultured rat cortical astroglia. *Channels* **3**, 323-336.

Boese, S. H., Wehner, F. and Kinne, R. K. (1996). Taurine permeation through swelling-activated anion conductance in rat IMCD cells in primary culture. *Am. J. Physiol.* **271**, F498-F507.

Bowens, N. H., Dohare, P., Kuo, Y.-H. and Mongin, A. A. (2013). DCPIB, the proposed selective blocker of volume-regulated anion channels, inhibits several glutamate transport pathways in glial cells. *Mol. Pharmacol.* **83**, 22-32.

Burow, P., Klapperstück, M. and Markwardt, F. (2015). Activation of ATP secretion via volume-regulated anion channels by sphingosine-1-phosphate in RAW macrophages. *Pflügers Arch* **467**, 1215-1226.

Chen, P. E., Geballe, M. T., Stansfeld, P. J., Johnston, A. R., Yuan, H., Jacob, A. L., Snyder, J. P., Traynelis, S. F. and Wyllie, D. J. (2005). Structural features of the glutamate binding site in recombinant NR1/NR2A N-methyl-D-aspartate receptors determined by site-directed mutagenesis and molecular modeling. *Mol. Pharmacol.* **67**, 1470-1484.

Choe, K. Y., Olson, J. E. and Bourque, C. W. (2012). Taurine release by astrocytes modulates osmosensitive glycine receptor tone and excitability in the adult supraoptic nucleus. *J. Neurosci.* **32**, 12518-12527.

Diaz, M. R., Wadleigh, A., Hughes, B. A., Woodward, J. J. and Valenzuela, C. F. (2011). Bestrophin1 channels are insensitive to ethanol and do not mediate tonic GABAergic currents in cerebellar granule cells. *Front. Neurosci.* **5**, 148.

Duan, S., Anderson, C. M., Keung, E. C., Chen, Y. and Swanson, R. A. (2003). P2X7 receptor-mediated release of excitatory amino acids from astrocytes. *J. Neurosci.* **23**, 1320-1328.

Fields, R. D. and Ni, Y. (2010). Nonsynaptic communication through ATP release from volume-activated anion channels in axons. *Sci. Signal.* **3**, ra73.

Franco, R., Torres-Marquez, M. E. and Pasantes-Morales, H. (2001). Evidence for two mechanisms of amino acid osmolyte release from hippocampal slices. *Pflügers Arch* **442**, 791-800.

Gaitán-Peñas, H., Gradogna, A., Laparra-Cuervo, L., Solsona, C., Fernández-Dueñas, V., Barrallo-Gimeno, A., Ciruela, F., Lakadamyali, M., Pusch, M. and Estévez, R. (2016). Investigation of LRRC8-mediated volume-regulated anion currents in *xenopus* oocytes. *Biophys. J.* **111**, 1429-1443.

Gosling, M., Smith, J. W. and Poyner, D. R. (1995). Characterization of a volume-sensitive chloride current in rat osteoblast-like (ROS 17/2.8) cells. *J. Physiol.* **485**, 671-682.

Hamilton, N. B. and Attwell, D. (2010). Do astrocytes really exocytose neurotransmitters? *Nat. Rev. Neurosci.* **11**, 227-238.

Harada, K., Kamiya, T. and Tsuboi, T. (2015). Gliotransmitter release from astrocytes: functional, developmental, and pathological implications in the brain. *Front. Neurosci.* **9**, 499.

Hazama, A., Shimizu, T., Ando-Akatsuka, Y., Hayashi, S., Tanaka, S., Maeno, E. and Okada, Y. (1999). Swelling-induced, CFTR-independent ATP release from a human epithelial cell line: lack of correlation with volume-sensitive Cl^- channels. *J. Gen. Physiol.* **114**, 525-533.

Hisadome, K., Koyama, T., Kimura, C., Droogmans, G., Ito, Y. and Oike, M. (2002). Volume-regulated anion channels serve as an auto/paracrine nucleotide release pathway in aortic endothelial cells. *J. Gen. Physiol.* **119**, 511-520.

Hussy, N., Deleuze, C., Pantaloni, A., Desarménien, M. G. and Moos, F. (1997). Agonist action of taurine on glycine receptors in rat supraoptic magnocellular neurones: possible role in osmoregulation. *J. Physiol.* **502**, 609-621.

Hussy, N., Deleuze, C., Desarménien, M. G. and Moos, F. C. (2000). Osmotic regulation of neuronal activity: a new role for taurine and glial cells in a hypothalamic neuroendocrine structure. *Prog. Neurobiol.* **62**, 113-134.

Hyzinski-García, M. C., Rudkouskaya, A. and Mongin, A. A. (2014). LRRC8A protein is indispensable for swelling-activated and ATP-induced release of excitatory amino acids in rat astrocytes. *J. Physiol.* **592**, 4855-4862.

Inoue, H. and Okada, Y. (2007). Roles of volume-sensitive chloride channel in excitotoxic neuronal injury. *J. Neurosci.* **27**, 1445-1455.
Inoue, H., Ohtaki, H., Nakamachi, T., Shioda, S. and Okada, Y. (2007). Anion channel blockers attenuate delayed neuronal cell death induced by transient forebrain ischemia. *J. Neurosci. Res.* **85**, 1427-1435.
Iwasa, K., Tasaki, I. and Gibbons, R. C. (1980). Swelling of nerve fibers associated with action potentials. *Science* **210**, 338-339.
Jackson, P. S. and Strange, K. (1993). Volume-sensitive anion channels mediate swelling-activated inositol and taurine efflux. *Am. J. Physiol.* **265**, C1489-C1500.
Jackson, P. S., Morrison, R. and Strange, K. (1994). The volume-sensitive organic osmolyte-anion channel VSOAC is regulated by nonhydrolytic ATP binding. *Am. J. Physiol.* **267**, C1203-C1209.
Jentsch, T. J. (2016). VRACs and other ion channels and transporters in the regulation of cell volume and beyond. *Nat. Rev. Mol. Cell Biol.* **17**, 293-307.
Kim, G. H., Kosterin, P., Obaid, A. L. and Salzberg, B. M. (2007). A mechanical spike accompanies the action potential in Mammalian nerve terminals. *Biophys. J.* **92**, 3122-3129.
Kimelberg, H. K., Goderie, S. K., Higman, S., Pang, S. and Waniewski, R. A. (1990). Swelling-induced release of glutamate, aspartate, and taurine from astrocyte cultures. *J. Neurosci.* **10**, 1583-1591.
Kubo, M. and Okada, Y. (1992). Volume-regulatory Cl– channel currents in cultured human epithelial cells. *J. Physiol.* **456**, 351-371.
Lambert, I. H. and Hoffmann, E. K. (1994). Cell swelling activates separate taurine and chloride channels in Ehrlich mouse ascites tumor cells. *J. Membr. Biol.* **142**, 289-298.
Le-Corronc, H., Rigo, J.-M., Branchereau, P. and Legendre, P. (2011). $GABA_A$ receptor and glycine receptor activation by paracrine/autocrine release of endogenous agonists: more than a simple communication pathway. *Mol. Neurobiol.* **44**, 28-52.
Lee, S., Yoon, B.-E., Berglund, K., Oh, S.-J., Park, H., Shin, H.-S., Augustine, G. J. and Lee, C. J. (2010). Channel-mediated tonic GABA release from glia. *Science* **330**, 790-796.
Lee, C. C., Freinkman, E., Sabatini, D. M. and Ploegh, H. L. (2014). The protein synthesis inhibitor blasticidin S enters mammalian cells via leucine-rich repeat-containing protein 8D. *J. Biol. Chem.* **289**, 17124-17131.
Manolopoulos, V. G., Voets, T., Declercq, P. E., Droogmans, G. and Nilius, B. (1997). Swelling-activated efflux of taurine and other organic osmolytes in endothelial cells. *Am. J. Physiol.* **273**, C214-C222.
Martineau, M., Parpura, V. and Mothet, J.-P. (2014). Cell-type specific mechanisms of D-serine uptake and release in the brain. *Front. Synaptic Neurosci.* **6**, 12.
Mongin, A. A. (2015). Volume-regulated anion channel-a frenemy within the brain. *Pflügers Arch* **468**, 421-441.
Mongin, A. A. and Kimelberg, H. K. (2002). ATP potently modulates anion channel-mediated excitatory amino acid release from cultured astrocytes. *Am. J. Physiol. Cell Physiol.* **283**, C569-C578.
Montero, T. D. and Orellana, J. A. (2015). Hemichannels: new pathways for gliotransmitter release. *Neuroscience* **286**, 45-59.
Mothet, J. P., Parent, A. T., Wolosker, H., Brady, R. O., Jr, Linden, D. J., Ferris, C. D., Rogawski, M. A. and Snyder, S. H. (2000). D-serine is an endogenous ligand for the glycine site of the N-methyl-D-aspartate receptor. *Proc. Natl. Acad. Sci. USA* **97**, 4926-4931.
Nilius, B., Eggermont, J., Voets, T., Buyse, G., Manolopoulos, V. and Droogmans, G. (1997). Properties of volume-regulated anion channels in mammalian cells. *Prog. Biophys. Mol. Biol.* **68**, 69-119.
Okada, Y. (1997). Volume expansion-sensing outward-rectifier Cl^- channel: fresh start to the molecular identity and volume sensor. *Am. J. Physiol.* **273**, C755-C789.
Orellana, J. A. and Stehberg, J. (2014). Hemichannels: new roles in astroglial function. *Front. Physiol.* **5**, 193.
Parpura, V., Basarsky, T. A., Liu, F., Jeftinija, K., Jeftinija, S. and Haydon, P. G. (1994). Glutamate-mediated astrocyte-neuron signalling. *Nature* **369**, 744-747.
Pasantes-Morales, H., Murray, R. A., Sánchez-Olea, R. and Morán, J. (1994). Regulatory volume decrease in cultured astrocytes. II. Permeability pathway to amino acids and polyols. *Am. J. Physiol.* **266**, C172-C178.
Patneau, D. K. and Mayer, M. L. (1990). Structure-activity relationships for amino acid transmitter candidates acting at N-methyl-D-aspartate and quisqualate receptors. *J. Neurosci.* **10**, 2385-2399.
Pedersen, S. F., Okada, Y. and Nilius, B. (2016). Biophysics and physiology of the volume-regulated anion channel (VRAC)/volume-sensitive outwardly rectifying anion channel (VSOR). *Pflügers Arch* **468**, 371-383.
Planells-Cases, R., Lutter, D., Guyader, C., Gerhards, N. M., Ullrich, F., Elger, D. A., Kucukosmanoglu, A., Xu, G., Voss, F. K., Reincke, S. M. et al. (2015). Subunit composition of VRAC channels determines substrate specificity and cellular resistance to Pt-based anti-cancer drugs. *EMBO J.* **34**, 2993-3008.
Prager-Khoutorsky, M. and Bourque, C. W. (2015). Mechanical basis of osmosensory transduction in magnocellular neurosecretory neurones of the rat supraoptic nucleus. *J. Neuroendocrinol.* **27**, 507-515.
Prager-Khoutorsky, M., Khoutorsky, A. and Bourque, C. W. (2014). Unique interweaved microtubule scaffold mediates osmosensory transduction via physical interaction with TRPV1. *Neuron* **83**, 866-878.
Qiu, Z., Dubin, A. E., Mathur, J., Tu, B., Reddy, K., Miraglia, L. J., Reinhardt, J., Orth, A. P. and Patapoutian, A. (2014). SWELL1, a plasma membrane protein, is an essential component of volume-regulated anion channel. *Cell* **157**, 447-458.
Rosenberg, D., Kartvelishvily, E., Shleper, M., Klinker, C. M. C., Bowser, M. T. and Wolosker, H. (2010). Neuronal release of D-serine: a physiological pathway controlling extracellular D-serine concentration. *FASEB J.* **24**, 2951-2961.
Sabirov, R. Z., Merzlyak, P. G., Islam, M. R., Okada, T. and Okada, Y. (2016). The properties, functions, and pathophysiology of maxi-anion channels. *Pflugers Arch.* **468**, 405-420.
Schmieden, V., Grenningloh, G., Schofield, P. R. and Betz, H. (1989). Functional expression in *Xenopus* oocytes of the strychnine binding 48 kd subunit of the glycine receptor. *EMBO J.* **8**, 695-700.
Shennan, D. B. (2008). Swelling-induced taurine transport: relationship with chloride channels, anion-exchangers and other swelling-activated transport pathways. *Cell. Physiol. Biochem.* **21**, 15-28.
Stutzin, A., Torres, R., Oporto, M., Pacheco, P., Eguiguren, A. L., Cid, L. P. and Sepúlveda, F. V. (1999). Separate taurine and chloride efflux pathways activated during regulatory volume decrease. *Am. J. Physiol.* **277**, C392-C402.
Syeda, R., Qiu, Z., Dubin, A. E., Murthy, S. E., Florendo, M. N., Mason, D. E., Mathur, J., Cahalan, S. M., Peters, E. C., Montal, M. et al. (2016). LRRC8 proteins form volume-regulated anion channels that sense ionic strength. *Cell* **164**, 499-511.
Ullrich, F., Reincke, S. M., Voss, F. K., Stauber, T. and Jentsch, T. J. (2016). Inactivation and anion selectivity of volume-regulated VRAC channels depend on carboxy-terminal residues of the first extracellular loop. *J. Biol. Chem.* **291**, 17040-17048.
Verkhratsky, A., Rodríguez, J. J. and Parpura, V. (2012). Neurotransmitters and integration in neuronal-astroglial networks. *Neurochem. Res.* **37**, 2326-2338.
Verkhratsky, A., Matteoli, M., Parpura, V., Mothet, J.-P. and Zorec, R. (2016). Astrocytes as secretory cells of the central nervous system: idiosyncrasies of vesicular secretion. *EMBO J.* **35**, 239-257.
Voss, F. K., Ullrich, F., Münch, J., Lazarow, K., Lutter, D., Mah, N., Andrade-Navarro, M. A., von Kries, J. P., Stauber, T. and Jentsch, T. J. (2014). Identification of LRRC8 heteromers as an essential component of the volume-regulated anion channel VRAC. *Science* **344**, 634-638.
Wolosker, H., Blackshaw, S. and Snyder, S. H. (1999). Serine racemase: a glial enzyme synthesizing D-serine to regulate glutamate-N-methyl-D-aspartate neurotransmission. *Proc. Natl. Acad. Sci. USA* **96**, 13409-13414.
Ye, Z.-C., Oberheim, N., Kettenmann, H. and Ransom, B. R. (2009). Pharmacological "cross-inhibition" of connexin hemichannels and swelling activated anion channels. *Glia* **57**, 258-269.
Yoon, B.-E., Woo, J., Chun, Y. E., Chun, H., Jo, S., Bae, J. Y., An, H., Min, J. O., Oh, S.-J., Han, K. S. et al. (2014). Glial GABA, synthesized by monoamine oxidase B, mediates tonic inhibition. *J. Physiol.* **592**, 4951-4968.
Zhang, Y., Zhang, H., Feustel, P. J. and Kimelberg, H. K. (2008). DCPIB, a specific inhibitor of volume regulated anion channels (VRACs), reduces infarct size in MCAo and the release of glutamate in the ischemic cortical penumbra. *Exp. Neurol.* **210**, 514-520.

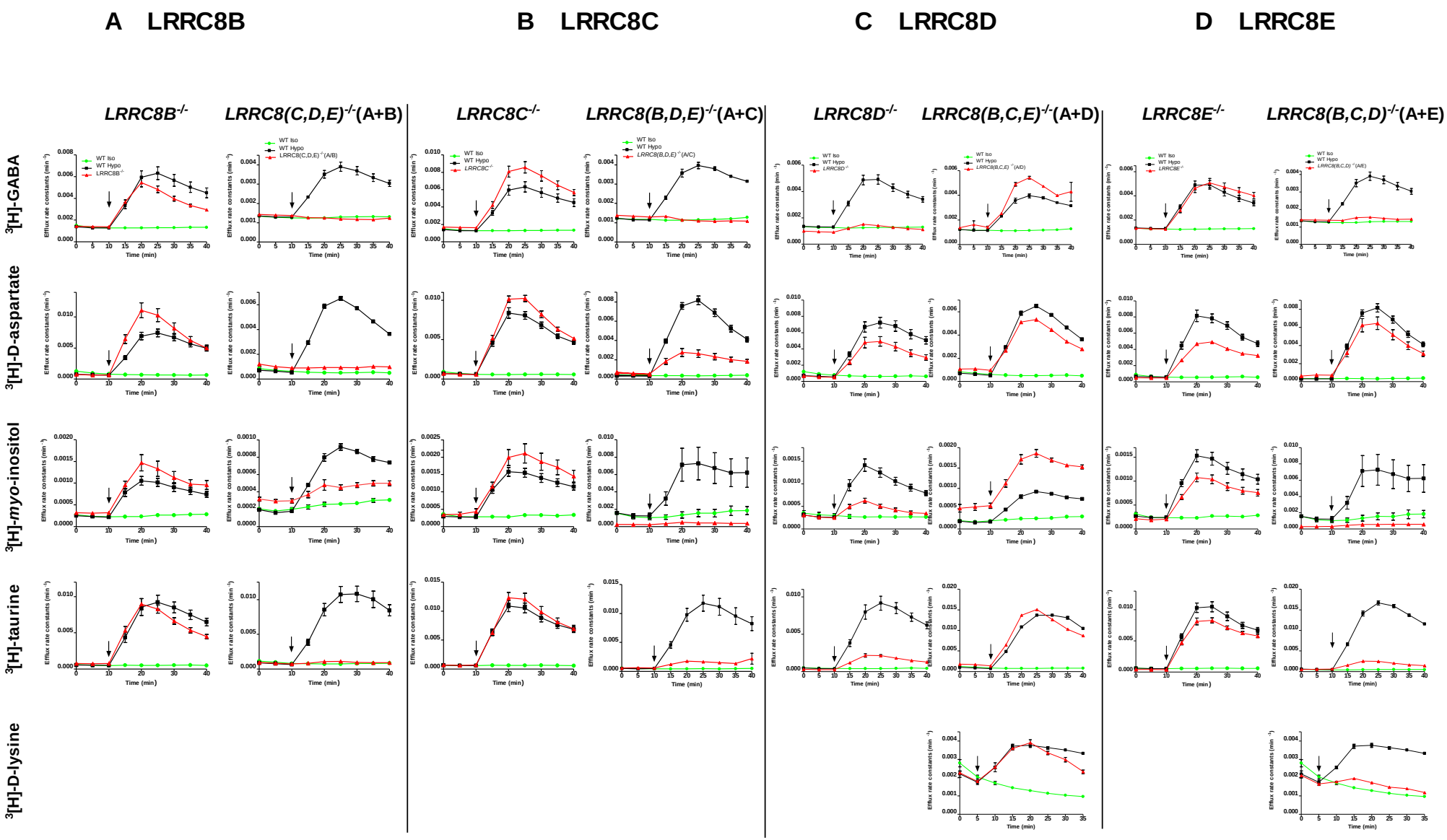

Journal of Cell Science • Supplementary information

Fig. S1: Efflux of organic VRAC substrates as function of LRRC8B-E subunits. Time course of swelling-induced efflux of radiolabeled organic compounds in HEK293 cells. (**A-D**) Efflux from cells in which single LRRC8 genes were disrupted (left panels), and from cells carrying disruptions in three LRRC8 genes, leaving only the obligatory LRRC8A and one other LRRC8 isoform (right panels) intact. Taurine efflux data shown for "*LRRC8D*$^{-/-}$", "A+C", "A+D", and "A+E" have been published previously (Planells-Cases et al., 2015) and are depicted again for comparison. Mean values of at least two independent experiments (n=4 per experiment), error bars=s.e.m.

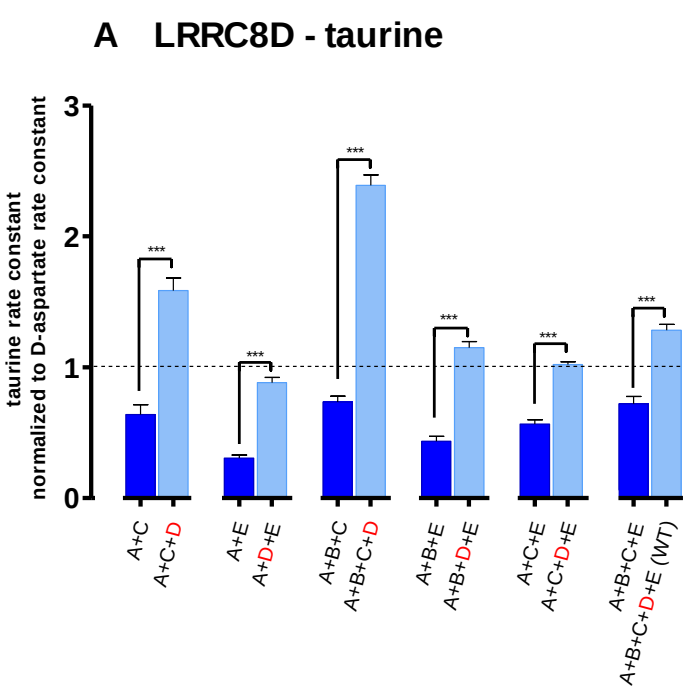
A LRRC8D - taurine
taurine rate constant
normalized to D-aspartate rate constant
A+C
A+C+D
A+E
A+D+E
A+B+C
A+B+C+D
A+B+E
A+B+D+E
A+C+E
A+C+D+E
A+B+C+E
A+B+C+D+E (WT)

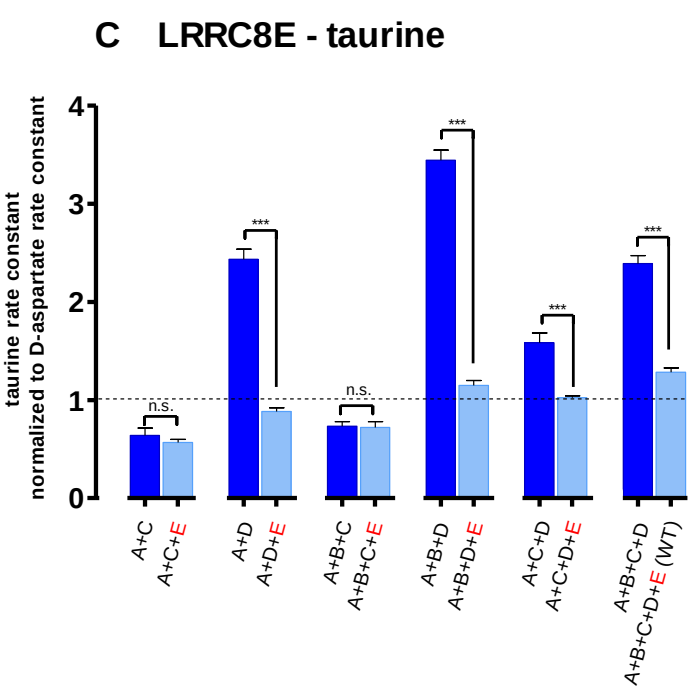
C LRRC8E - taurine
taurine rate constant
normalized to D-aspartate rate constant
n.s.
A+C
A+C+E
A+D
A+D+E
A+B+C
A+B+C+E
A+B+D
A+B+D+E
A+C+D
A+C+D+E
A+B+C+D
A+B+C+D+E (WT)

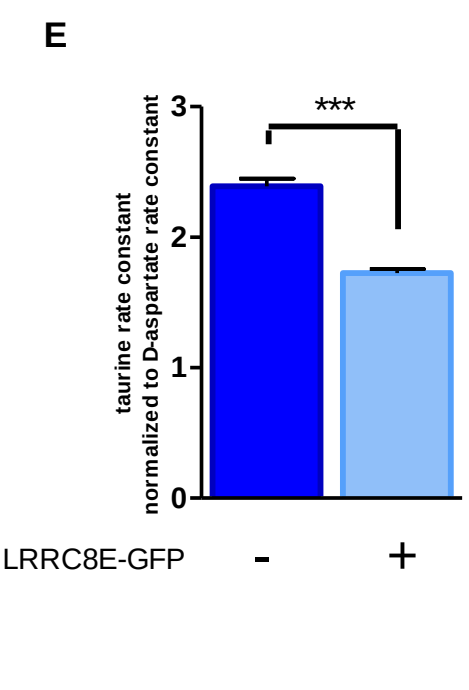
E
taurine rate constant
normalized to D-aspartate rate constant
LRRC8E-GFP
-
+

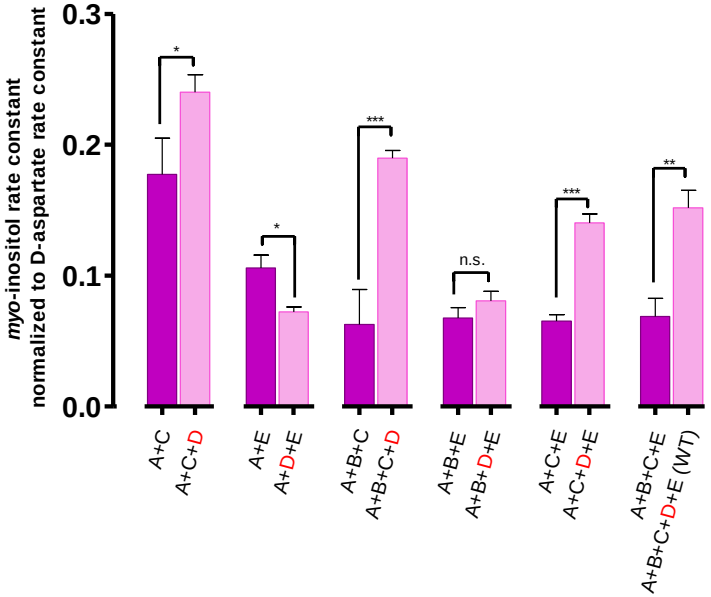
B LRRC8D - myo-inositol
myo-inositol rate constant
normalized to D-aspartate rate constant
n.s.
A+C
A+C+D
A+E
A+D+E
A+B+C
A+B+C+D
A+B+E
A+B+D+E
A+C+E
A+C+D+E
A+B+C+E
A+B+C+D+E (WT)

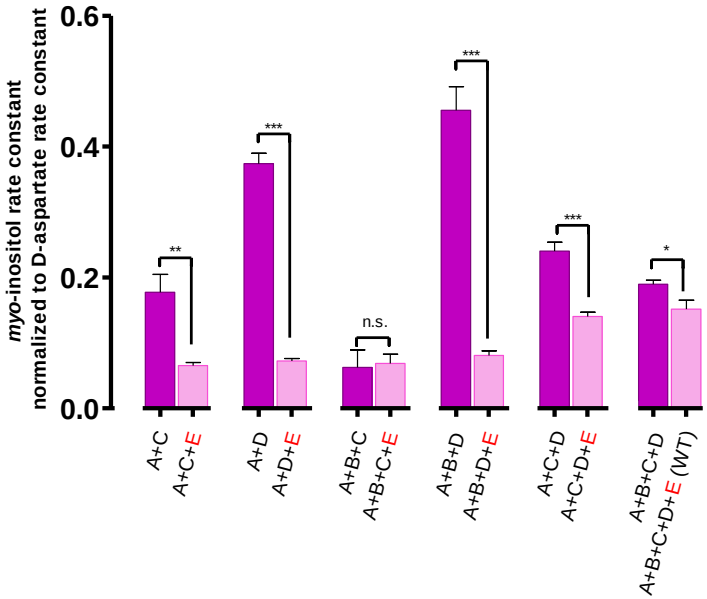
D LRRC8E - myo-inositol
myo-inositol rate constant
normalized to D-aspartate rate constant
n.s.
A+C
A+C+E
A+D
A+D+E
A+B+C
A+B+C+E
A+B+D
A+B+D+E
A+C+D
A+C+D+E
A+B+C+D
A+B+C+D+E (WT)

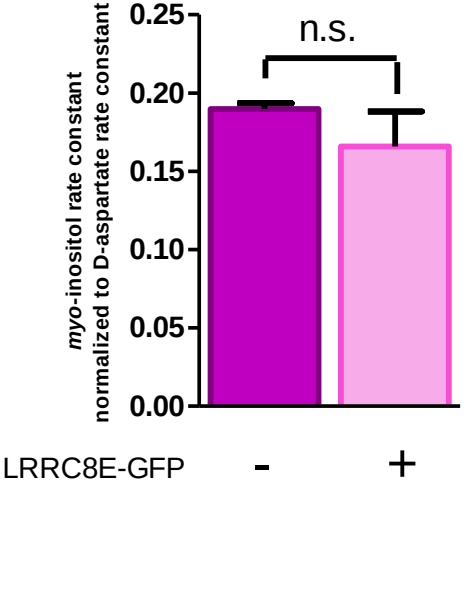
F
myo-inositol rate constant
normalized to D-aspartate rate constant
n.s.
LRRC8E-GFP
-
+

Fig. S2: Effect of inclusion of LRRC8D or LRRC8E on apparent substrate selectivity of VRAC. Influence of additional expression of LRRC8D (**A, B**) or LRRC8E (**C, D**) on ^{3}[H]-taurine (**A, C**) or ^{3}[H]-*myo*-inositol (**B, D**) over ^{3}[H]-D-aspartate transport ratios. Ratios of respective maximal rate constants are depicted as bars which are grouped to easily compare HEK293 clones lacking (dark bars) or expressing (light bars) LRRC8D or LRRC8E, respectively. Experiments used various KO cell lines in which all LRRC8 subunits are expressed from endogenous promotors. **(E, F)** Effect of transiently transfected LRRC8E (light bars) on ^{3}[H]-taurine (**E**) and ^{3}[H]-*myo*-inositol (**F**) over ^{3}[H]-D-aspartate efflux ratio in *LRRC8E*$^{-/-}$ HEK293 cells. Mean values of two independent experiments (n=4 each for each substrate), error bars=s.e.m. *P ≤ 0.05; **P ≤ 0.01; and ***P ≤ 0.001 (Mann-Whitney test).

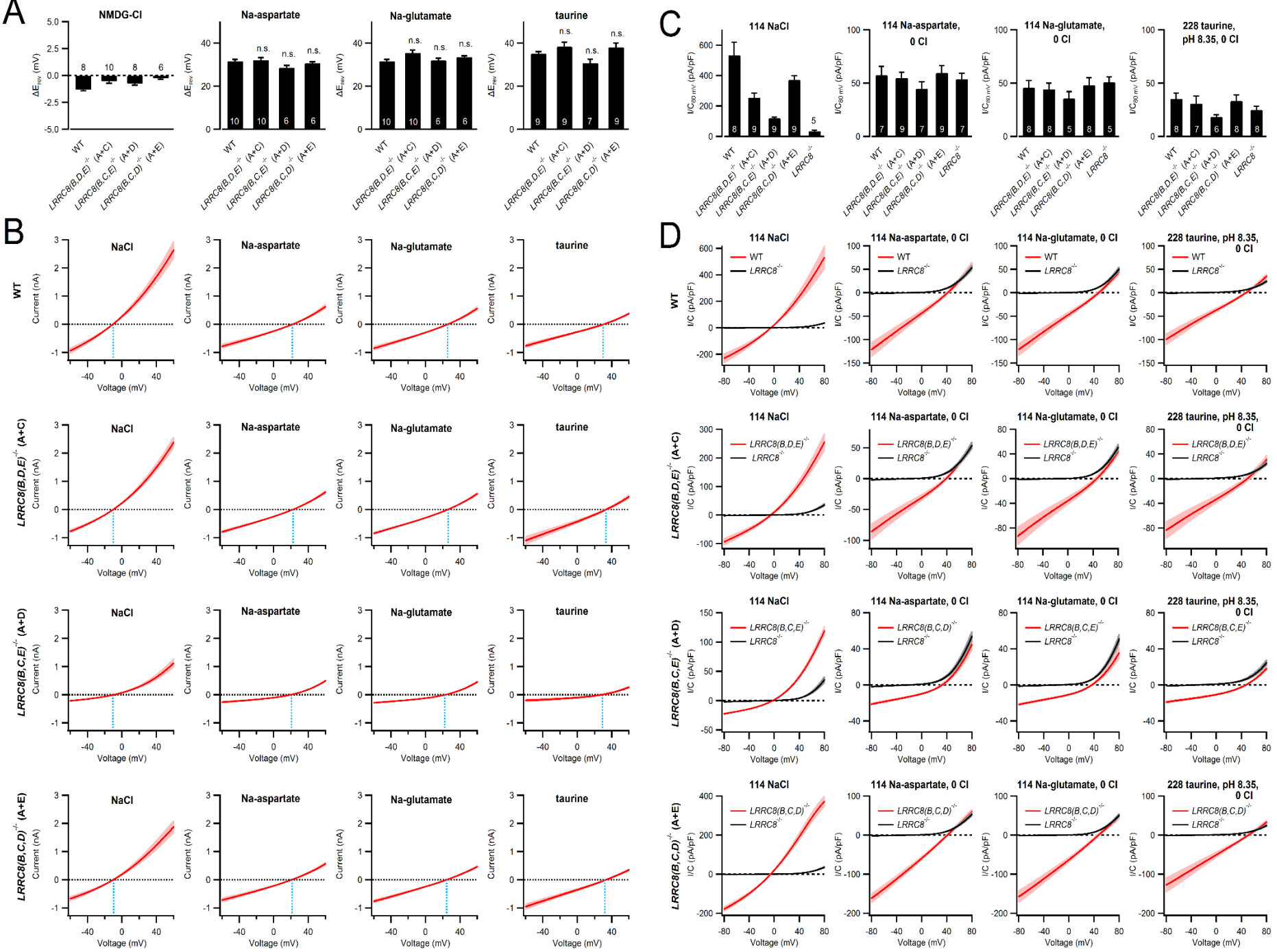

Fig. S3: Whole-cell patch recordings of amino acid currents in different HEK293 *LRRC8* knockout clones. (A) Relative shifts in reversal potential (ΔE_{rev}) of fully activated $I_{Cl,vol}$ in different HEK293 *LRRC8* knockout cell lines upon equimolar substitution of NaCl in the standard hypotonic bath solution (105 mM) with the indicated substances. All bath solutions additionally contained 11 mM Cl^- (see Methods). The taurine bath solution contained 210 mM taurine at pH 8.35. Assuming a pK_a value of 8.74 (The Merck Index, 12th ed., Entry# 9241.), the concentration of anionic taurine was ~61 mM. Values from knockout cell lines were compared to WT values using one-way ANOVA and Bonferroni's test. Bars are mean ± s.e.m. n is indicated. Data are corrected for differing liquid junction potentials. **(B)** Averaged $I_{Cl,vol}$ traces in response to 2-s-voltage ramps from -60 to 60 mV in the indicated cell lines with the indicated extracellular charge carriers. Dashed blue lines indicate reversal potentials. Liquid junction potentials were not corrected. The sweep width represents mean ± s.e.m. **(C)** Current densities at 80 mV (I/C) of swelling-activated currents from different HEK293 *LRRC8* knockout cell lines with the indicated anionic charge carriers in the bath solutions. No additional Cl^- was present (see Methods). The taurine solution contained ~66 mM anionic taurine assuming a pK_a of 8.74. Bars are mean ± s.e.m. n is indicated. **(D)** Averaged current density traces in response to 2-s-voltage ramps from -80 to 80 mV in the indicated cell lines with the indicated extracellular charge carriers. The sweep width represents mean ± s.e.m. Liquid junction potentials were not corrected.

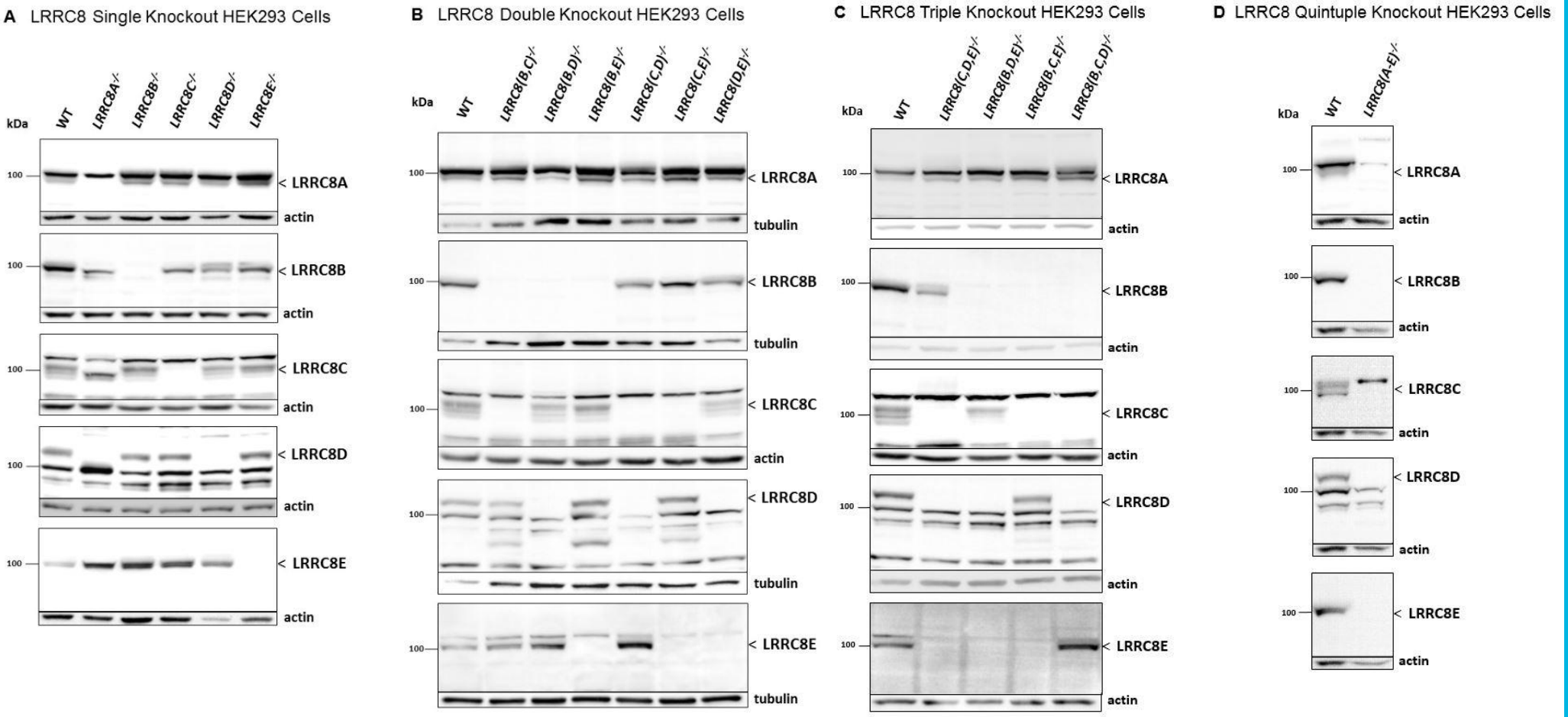

Fig. S4: LRRC8 subunit expression in different HEK293 LRRC8 knockout clones. Western blots showing the expression of LRRC8A through LRRC8E in single (**A**), double (**B**), triple (**C**) and quintuple (**D**) *LRRC8* knockout clones. Specific bands are marked by black arrows. Tubulin or actin served as loading control. Note that absence of LRRC8A (**A**) leads to size shift of the other LRRC8 subunits, which cannot leave the ER without LRRC8A and are thus differently glycosylated.

Supplemental Table S1. Monoclonal HEK293 cell lines with *LRRC8* gene disruption

HEK293 cell line	Clone name	Construct used*	Genetic modification	Used for Figure
***LRRC8A*$^{-/-}$**	3E7	3A	a1: Δ21nt (T110-A130) a2: insertion of 1 nt (T after C123)	1A/B/G, 2A/B
	1.13	3A	homozygous insertion of 55 nt (after T121)	1C/E/F, 2A/B, 6C, S4A
	1.6	3A	Homozygous net Δ13 nt (within A37-G138)	1D, 2A,B
***LRRC8B*$^{-/-}$**	B1	2B	a1: Δ1nt (A449) a2: Δ25nt (G443-T467) a3: Insertion of 1 nt (T after C445)	2A, 4A-D, 6A/C, S2A-D, S4A
***LRRC8C*$^{-/-}$**	C3	1C	homozygous duplication of T119	2A, 4A-D, 6A/C, S2A-D, S4A
***LRRC8D*$^{-/-}$**	Dn3	1D	a1: duplication of A325 a2: Δ4nt (T321-C324) a3: Δ5nt (A325-C329)	2A, 4A-D, 6A/C, S2A-D, S4A
***LRRC8E*$^{-/-}$**	E2	1E	a1: deletion 1 nt (A94) a2: duplication of A94	2A, 4A-D, 6A/C, S2A-F, S4A
***LRRC8(B,C)*$^{-/-}$**	(1)A10	2B, 1C	B: a1: duplication of T446 B: a2: Δ14 nt (C435-G448) C: homozygous duplication of T119	3A, 4A-D, 6D, S2A-D, S4B
***LRRC8(B,D)*$^{-/-}$**	(2)E12	2B, 1D	B: a1: Δ7nt (G444-G450) a2: insertion of 1 nt (T after C445) D: a1: duplication of A325 a2: Δ4nt (T321-C324) a3: Δ5nt (A325-C329)	4A-D, 6D, S2A-D, S4B
***LRRC8(B,E)*$^{-/-}$**	(3)A3	2B, 1E	B: a1: Δ1nt (A449) a2: Δ25nt (G443-T467) a3: Insertion of 1 nt (T after C445) E: homozygous Δ 5 nt (T92-C96)	4A-D, 6D, S2A-D, S4B
***LRRC8(C,D)*$^{-/-}$**	(4)E2	1C, 1D	C: homozygous duplication of T119 D: a1: insertion of one nt (A after C324) a2: Δ5nt (deletion G322-C328 and insertion of GG)	4A-D, 6D, S2A-D, S4B
***LRRC8(C,E)*$^{-/-}$**	(5)A6	1C, 1E	C: homozygous duplication of T119 E: homozygous duplication of A94	4A-D, 6D, S2A-D, S4B
***LRRC8(D,E)*$^{-/-}$**	(6)E5	1D, 1E	D: a1: duplication of A325 a2: Δ4nt (T321-C324) a3: Δ5nt (A325-C329) E: homozygous duplication of A94	3B, 4A/B, 6D, S2A-D, S4B
***LRRC8(C,D,E)*$^{-/-}$**	3.6	1C, 1D, 1E	C: homozygous duplication of T119 D: homozygous duplication of A325 E: homozygous duplication of A95	2B, 6B/E, S4C
***LRRC8(B,C,D)*$^{-/-}$**	4.1	2B, 1C, 1D	B: homozygous insertion of 2 nt (TT after A430) C: homozygous duplication of T119 D: homozygous duplication of A325	2B, 4A-D, 6B/E, S2A/B, S3, S4C
***LRRC8(B,C,E)*$^{-/-}$**	5.5	2B, 1C, 1E	B: a1: duplication of T433 a2: Δ13nt (A433-C445) a3: Δ5nt (C445-A449) C: homozygous duplication of T119 E: a1: duplication of A94 a2: Δ2nt (C95-C96) a3: Δ8nt (A94-C101)	2B, 4A-D, 6B/E, S2C/D, S3, S4C
***LRRC8 (B,D,E)*$^{-/-}$**	6.3	2B, 1D, 1E	B: homozygous Δ2nt (T446-C447) D: homozygous duplication of A325 E: a1: deletion 1 nt (A94) a2: duplication of A94	2B, 4A/B, 6B/E, S2A-D, S3, S4C
***LRRC8(A,B,C,D,E)*$^{-/-}$**	5xKO A4	3A, 2B, 1C, 1D, 1E	A: a1: Δ14nt (C116-G129) a2: Δ2nt (deletion G125-G129, insertion AAG) B: homozygous insertion of 2 nt (TT after A430) C: homozygous duplication of T119 D: homozygous duplication of A325 E: a1: duplication of A94 a2: deletion 1 nt (A94)	5, 6E, S3C/D, S4D

Journal of Cell Science • Supplementary information

Supplemental Table S2. SgRNA used for CRISPR/Cas9-guided LRRC8 gene disruption in HEK293 cells

Target gene	Construct	Guide sequence (5´→3´)	Targeting strand	Target location in protein
LRRC8A	3A	tgatgattgccgtcttcgggggg	+	aa 36-43 (in TMD1)
LRRC8B	2B	ggccacaaaatgctcgagcctgg	-	aa 147-154 (between TMD2 and TMD3)
LRRC8C	1C	atgctcatgatcggcgtgtttgg	+	aa35-42 (in TMD1)
LRRC8D	1D	gtggctctgagaggtatgtcagg	-	aa107-114 (between TMD1 and TMD2)
LRRC8E	1E	gctggccgagtacctcaccgtgg	+	aa26-34 (in TMD1)

TMD = transmembrane domain. aa = amino acid. PAM sequence is underlined